pharmaceuticals

MDPI

Review

Small-Molecule Fluorescent Probe for Detection of Sulfite

Ting Li, Xuyang Chen, Kai Wang * and Zhigang Hu *

Medical Laboratory of Wuxi Children's Hospital, The Affiliated Wuxi People's Hospital of Nanjing Medical University, Qingyang Road 299, Wuxi 214023, China
* Correspondence: hyxj0309@163.com (K.W.); jswxhzg@163.com (Z.H.)

Abstract: Sulfite is widely used as an antioxidant additive and preservative in food and beverages. Abnormal levels of sulfite in the body is related to a variety of diseases. There are strict rules for sulfite intake. Therefore, to monitor the sulfite level in physiological and pathological events, there is in urgent need to develop a rapid, accurate, sensitive, and non-invasive approach, which can also be of great significance for the improvement of the corresponding clinical diagnosis. With the development of fluorescent probes, many advantages of fluorescent probes for sulfite detection, such as real time imaging, simple operation, economy, fast response, non-invasive, and so on, have been gradually highlighted. In this review, we enumerated almost all the sulfite fluorescent probes over nearly a decade and summarized their respective characteristics, in order to provide a unified platform for their standardized evaluation. Meanwhile, we tried to systematically review the research progress of sulfite small-molecule fluorescent probes. Logically, we focused on the structures, reaction mechanisms, and applications of sulfite fluorescent probes. We hope that this review will be helpful for the investigators who are interested in sulfite-associated biological procedures.

Keywords: fluorescent probes; sulfite detection; small-molecule; reaction mechanisms

Citation: Li, T.; Chen, X.; Wang, K.; Hu, Z. Small-Molecule Fluorescent Probe for Detection of Sulfite. *Pharmaceuticals* **2022**, *15*, 1326. https://doi.org/10.3390/ph15111326

Academic Editor: Thierry Besson

Received: 28 September 2022
Accepted: 22 October 2022
Published: 26 October 2022

1. Introduction

SO_2 is one of the main pollutants in the environment, and SO_2 derivatives are a collective term for SO_2 in its state of existence in living organisms, mainly in the form of sulfite (SO_3^{2-}) and bisulfite (HSO_3^-) in a neutral environment [1,2]. Sulfites are widely used as an antioxidant additive and preservative in food and beverages [3–6]. On the other hand, in living organisms, sulfur-containing amino acids are metabolized to produce endogenous sulfites [7]. Abnormal endogenous or exogenous sulfite levels have been reported to be associated with certain diseases, such as asthma, dyspnea, chest tightness, respiratory arrest, anaphylaxis, diarrhea, hypotension, migraine, stroke, brain cancer, lung cancer, and liver cancer [8–10]. According to the Joint FAO/WHO Expert Committee on Food, the daily intake of sulfites is limited to 0.7 mg/kg body weight [11,12]. The U.S. Food and Drug Administration (FDA) has stipulated that the level of sulfites in food and beverages should not exceed 125 μM [13]. The Chinese Hygienic Standard for the Use of Food Additives stipulates that in terms of SO_2 content, cookies, sugar, vermicelli, and canned foods shall not exceed 0.05 g/kg and other varieties shall not exceed 0.1 g/kg [14].

In recent years, numerous scholars have become interested in the effects of sulfites on living organisms. A study by Dalaman [15] et al. found that SO_2 significantly prevented the prolongation of QT interval and action potential duration in rats after isoproterenol induction. SO_2 derivatives inhibit the proliferation of human skin stratum corneum-forming cells by inhibiting the ERKI/2 and P38 pathways through activation of the NF–κB pathway [16]. Macrophage-derived SO_2 is an important regulator of macrophage activation, and it acts as an endogenous "switch" in the control of macrophage activation [17,18]. Therefore, it is necessary to develop easy-to-operate, efficient, and inexpensive methods for the detection of sulfites. There are many methods for the detection of sulfites, such as chromatography, electrochemistry, capillary electrophoresis, flow injection analysis, and

chemiluminescence [19]. However, these methods usually require complex procedures, and expensive instrumentation, and do not accurately assess sulfite fluctuations in biological systems. In contrast, fluorescence spectroscopy has the advantages of fast response, high sensitivity, simple operation, low cost, and in situ bioimaging within living cells for the detection of sulfites.

In the last decade, fluorescent probes have been used for the detection of various anions [20], such as ClO^-, Cl^-, $NO_2{}^-$, F^-, CN^-, S^{2-}, Br^-, etc [21–27]. In 2010, Choi et al. reported the first fluorescent probe for sulfite [28]. This research has attracted the attention of more and more researchers, and the construction of sulfite fluorescent probes is gradually becoming a popular research direction. Up to the present position, the number of research papers per year has increased dramatically, but there are few comprehensive reviews on small-molecule fluorescent probes for sulfite monitoring and applications. In this paper, we summarize the research progress of small-molecule fluorescent probes on sulfite in the last decade. In addition, this paper classifies sulfite fluorescent probes, including reaction mechanisms and constituent materials. We hope that this review will be useful for researchers who are interested in sulfite-related biological processes.

The design principle of sulfite fluorescent probes is related to their nucleophilic nature, where sulfite can undergo nucleophilic addition reactions with aldehyde groups or the deprotection of levulinic acid changes the probe structure causing changes in fluorescence spectra. A typical sulfite fluorescent probe consists of the three following main components: a fluorescent group, a recognition group, and a linker. Several important fluorophore of sulfite fluorescent probes are listed in this paper, including benzothiazole, coumarin, hemicyanine, quinoline, naphthalimide, benzimidazole, imidazole, triphenylamine, thiophene, pyrene, julolidine, Ir(III) complex, naphthalimide, rhodamine, flavor, which are further subdivided according to the mechanisms.

At present, the response types of these fluorescent probes are mainly classified into "turn-on" and "ratiometric" strategies. With sulfite, the main mode of the turn-on strategies is the switching on and enhancement of the fluorescence signal. In recent years, more and more fluorescent probes are of the ratiometric strategies, because compared to single-emission turn-on probes, ratiometric probes can achieve precise detection by the ratio of the two emitted signals, effectively mitigating conditions, concentrations, and instrumentation using self-calibration. The ratiometric probes can achieve accurate detection by the ratio of the two emitted signals and effectively mitigate the interference of conditions, concentrations, and instruments by self-calibration [29,30].

2. Small-Molecule Sulfite Fluorescent Probe

2.1. Based on Benzothiazole Fluorophore

Benzothiazole prolongs cellular conjugation π, increases cellular water solubility, and contributes to the selective aggregation of probes in cellular mitochondria. Benzothiazole functionalization greatly improves the analytical performance by increasing the quantum yield, emission band red shift, and introducing a second emission band [31]. We classified benzothiazole fluorophore into the following categories based on the mechanism including intramolecular charge transfer (ICT), excited state intramolecular proton transfer (ESIPT), and fluorescence resonance energy transfer (FRET).

2.1.1. ICT Mechanisms

ICT is the most common mechanism in fluorescent probes. The ICT mechanism refers to the process by which, in the excited state, the molecule will produce an electron transfer, resulting in the separation of the positive and negative charges. Generally, probes containing the ICT mechanism contain a push–pull system, i.e., "D–π–A" structure: where D (Donor) represents the electron donor and A (Acceptor) represents the electron acceptor, the electron transfer channel is provided by the π bond, and the final conjugated system is formed, and the electron donor or electron acceptor is the recognition group or part of the recognition group. When the probe reacts with the specific substrate, the electron donor or

electron acceptor of the recognition group will change, resulting in a push-pull system and the π electron structure in the system is rearranged, resulting in the red shift or blue shift phenomenon of the fluorescence spectrum. We have developed probes **1**–**5** based on ICT mechanisms, of which probe **1** was the turn-on type and probes **2**–**5** were the ratiometric type. Probe **2** was reversible, probe **3** was mitochondrial-targetable, and probe **5** detects both F^- and SO_3^{2-} (Scheme 1).

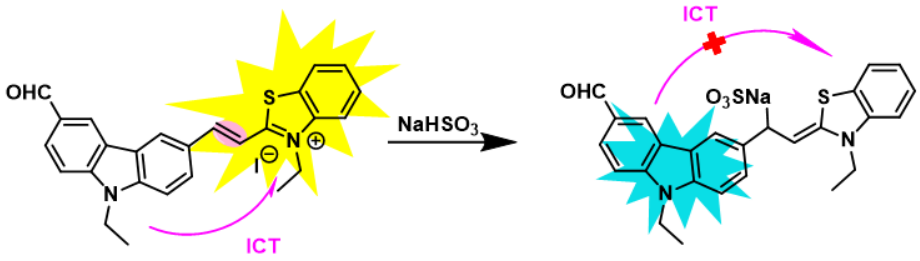

Scheme 1. Schematic diagram of ICT.

Probes **1**–**3** are capable of visualizing the detection of HSO_3^- and SO_3^{2-}. The addition of HSO_3^-/SO_3^{2-} activates the Michael receptor of probe **1** [32], disrupting the π-electron conjugation system and changing the solution color from purplish red to colorless. Meanwhile, probe **1** was successfully applied to detect SO_3^{2-}/HSO_3^- in real samples and HeLa cells. In contrast to probe **1**, probe **2** can reversibly monitor intracellular SO_3^{2-}/HSO_3^- [33]. Probe **2** itself showed near-infrared fluorescence emission at 630 nm, and the addition of SO_3^{2-}/HSO_3^- caused a gradual decrease in fluorescence intensity at 630 nm, but a significant enhancement of fluorescence at 630 nm was observed after the addition of H_2O_2, which was effective in restoring the system. To promote the application, the authors successfully used to monitor the redox process in cells and zebrafish. Compared with probe **2**, probe **3** [34] has a lower detection limit and enables the detection of SO_2 derivatives in various environments. Moreover, a comparative analysis of snow water and industrial wastewater revealed severe SO_2 contamination, and probe **3** has monitored the uptake, transport, and intracellular processes of exogenous HSO_3^- within the HeLa cell successfully.

The large Stokes shift can well separate the excitation and emission light and improve the sensitivity of fluorescence detection while reducing interference. Probe **4** [35] showed a large Stokes shift before and after the addition of SO_3^{2-}, based on the large Stokes shift after excitation of the fluorophore of benzothiazole derivatives due to the ESIPT process. Previous studies—because the introduction of the sensing group into the hydroxyl group—inhibited the ESIPT, so that the Stokes shift was reduced, so probe **4** added an aldehyde group as the reactive site for SO_3^{2-}, so the measurement process before and after the addition of SO_3^{2-} had a large Stokes displacement. Importantly, the probe has good selectivity for SO_3^{2-} and biothiols.

Qi [36] et al. developed a ratiometric fluorescent probe **5** capable of detecting both F^- and SO_3^{2-}. Probe **5** has the two following sensing groups: the tert-butyldimethylsilyl ether moiety of F^- and the carbon–carbon double bond of SO_3^{2-}. Emission titration experiments performed found that the addition of F^- enhanced the fluorescence intensity ratio of the probe by 291-fold, while the addition of SO_3^{2-} enhanced the fluorescence intensity ratio of the probe by 9445-fold. The authors suggest that the fluorescence is blue shifted by the weakening of ICT through Michael addition reaction between SO_3^{2-} and carbon–carbon double bond. However, the proposed mechanism lacks a theoretical basis. Thus, Jia [37] and her team in a study published in 2021 revealed the detection mechanism of probe **5** for F^- and SO_3^{2-} by density general function theory and time-varying density general function theory calculations, and the fluorescence red shift of the probe after the addition of F^- was caused by ESIPT, while the fluorescence blue shift of the probe after the addition of SO_3^{2-} was caused by ICT.

2.1.2. ESIPT Mechanisms

Excited state intramolecular proton transfer is the process of transferring intramolecular protons between a donor and an acceptor after the probe is excited. Molecules containing the ESIPT mechanism in general usually have amino and hydroxyl groups as proton donors, which are linked to neighboring proton acceptors (mostly S, N, and O atoms) through hydrogen bonds (Scheme 2). After the proton transfer, a more stable molecule is formed and the molecular structure is usually changed from enol to ketone, and the fluorescence spectrum is changed accordingly. Generally, for substances that can undergo intramolecular proton transfer, there is often a significant Stokes shift in the fluorescence emission peak of the substance, which effectively reduces background interference.

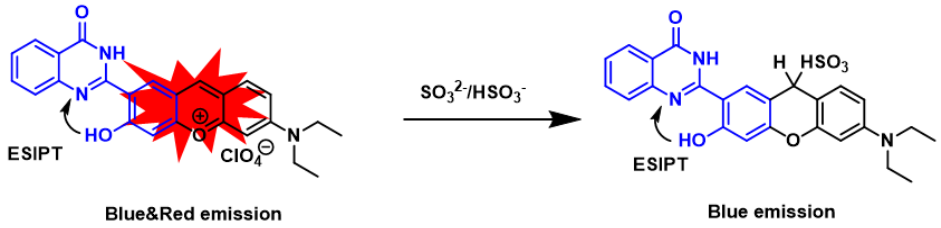

Scheme 2. Mechanism diagram of ESIPT.

Benzothiazole and its derivatives are the best-known ESIPT dyes, and the relative intensity variations of their photovariant isomers are often cleverly applied in the construction of scaled fluorescent probes. The emission of benzothiazole is usually confined to the blue and green regions and rarely exceeds 600 nm, and a straightforward way to obtain red shifted emission is to extend the *p*-conjugation of the ESIPT fluorophore. Zhang [38] et al. constructed probe **6** by combining benzothiazole with indole via C=C. This design extended the *p*-conjugated structure of benzothiazole and showed a larger red shift in both absorption and emission spectra compared with benzothiazole alone. After the addition of HSO_3^-, a rapid and significant change in the fluorescence spectrum was observed. Importantly, probe **6** can detect HSO_3^- in food and HeLa cells. Probe **7** [39] has a similar structure and sensing mechanism to probe **6**, a conjugate of benzothiazole and semicarbazide. Probe **7** is more suitable for sensing intracellular SO_3^{2-} and successfully detected SO_3^{2-} in MCF-7 cells.

In 2021, Zhu's [40] group constructed a benzothiazole-based probe **8**. The experimental results show that probe **8** has high application in HeLa cells and mice because it can detect endogenous SO_2. Moreover, it provides a reliable non-invasive method for visualizing SO_2 in mouse models during oxidative stress. More noteworthy is that probe **8** responds instantaneously (10 s) to sulfite.

2.1.3. FRET Mechanisms

Fluorescent probes based on fluorescence resonance energy transfer generally contain two fluorescent groups (energy donor D and energy acceptor A, respectively). If D is used to excite the whole system, the transfer process of energy from D to A will occur, and finally, the fluorescence of A will be presented. The following several elements must be present in a probe with a FRET mechanism: (1) The fluorophore as the energy donor, whose fluorescence emission is generally at a short wavelength, and the absorption spectrum of the fluorophore as the acceptor must overlap the emission spectrum of the donor fluorophore so that the acceptor fluorophore can absorb the energy of the energy donor at the emission wavelength. (2) The collision diameter between the energy donor and the energy acceptor must be much smaller than the distance between the donor and the acceptor. (3) The arrangement of the energy donor and the energy acceptor must be appropriate (Scheme 3).

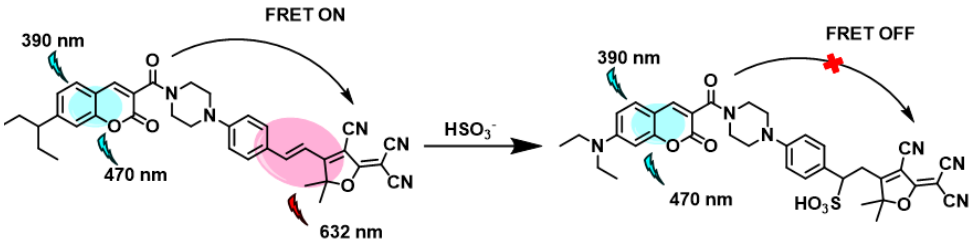

Scheme 3. Schematic diagram of principle FRET.

A ratiometric fluorescent probe **9**–**11** was developed based on benzothiazole fluorophore and FRET mechanisms and was able to detect the amount of HSO_3^- in MCF-7 cells. In 2014, probe **9** [41] was designed using benzothiazole and coumarin as fluorophores and was able to detect HSO_3^- concentrations between 0.934 and 100.0 mM. The experimental results revealed that the ratio of fluorescence intensity when the probe reacted with HSO_3^- increased continuously with increasing pH in the range of pH 5–8, which is due to the hydrolysis of coumarin under alkaline conditions. To overcome this obstacle, in 2016, Zhang [31] et al. designed probe **10** based on benzothiazole and anthocyanine dyes as fluorophores, which can react with HSO_3^- in PBS solvent, but the response of probe **10** to HSO_3^- takes 15 min, LOD = 340 nM. Wang's [42] group optimized and introduced TCF with strong electron-absorbing properties to combine with benzothiazole, which can detect HSO_3^- in the range of 5–40 μM, and the response time of probe **11** with HSO_3^- is only 3 min with LOD = 101 nM (Scheme 4).

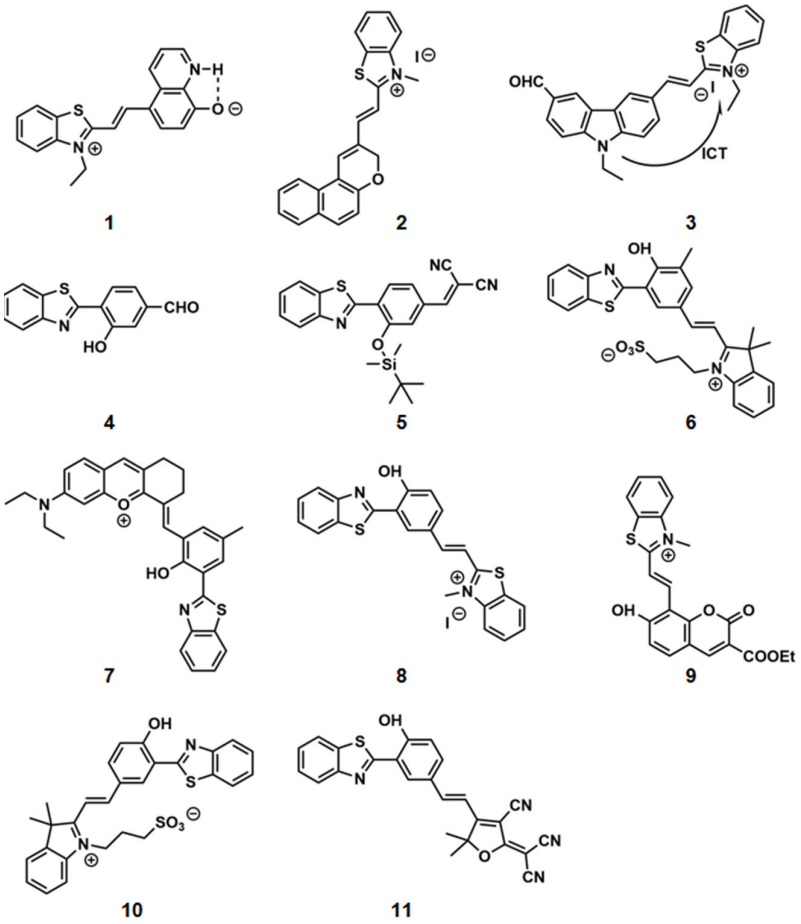

Scheme 4. The structures of sulfite fluorescent probes **1**–**11**.

2.2. Based on Coumarin Fluorophore

Coumarin was selected as a fluorophore due to its large Stokes shift, good solubility, high quantum yield, and excellent push–pull electron system. In the literature of the last 10 years summarized by me, the study of coumarin as a probe for fluorophores was mainly focused on 5 years ago. We classified coumarin fluorophore into the following categories based on the mechanism including intramolecular charge transfer (ICT), photon-induced electron transfer (PET), and fluorescence resonance energy transfer (FRET).

2.2.1. ICT Mechanisms

Based on ICT mechanisms, probes **12**–**22** were developed. Among them, probes **13**, **16**, and **19** are turn-on probes, and probes **12**, **14**–**15**, **17**–**18**, and **20**–**22** are ratiometric. Probes **20**–**22** can localize to mitochondria, and probes **15**–**16** are mainly dedicated to distinguishing sulfites from sulfides.

In 2013, Sun [43] et al. designed probe **12** based on the addition-rearrangement cascade reaction, which reacted with sulfite and increased the emission ratio by about 1110-fold, but the probe could not react with HSO_3^- in one step, the reaction time required 5 min, and the detection limit was 380 nM. Due to the slow response time, the maximum emission wavelength of the probe gradually changes, which is not suitable for real time detection of sulfite content in cells. So in 2015, Wang's [44] team made an improvement and designed probe **13**, which incorporates an electron-withdrawing group (-CN) to accelerate the reaction with SO_2 derivatives by activating carbon–carbon double bonds, so that the reaction is completed within 1 min.

The hydrophobic and alkaline microenvironment provided by the cationic surfactant micelles made the reaction of the probes with sulfite possible in an aqueous solution, thanks to the inspiration of Adamo and his colleagues' research. Therefore, Tian and his team [45] designed and synthesized three kinds of probes **14** (as show in Scheme 5) and used CTAB micelles to assist the reaction of the probes with sulfite.

Comparative experiments conducted found that the probe did not respond to sulfite after 20 h in the absence of CTAB and that the probe had poor selectivity (mainly HS^- and GSH had some effect on the detection) and a long reaction time. To solve the drawback of poor selectivity, next Tian and his team [46,47] designed probe **15** to distinguish sulfite from sulfide. Probe **15** covalently binds para-azidobenzenyl ketone to coumarin via a carbon–carbon double bond, distinguishing sulfite from sulfide by the different reaction sites (sulfite reacts with carbon–carbon double bond, sulfide reacts with azide group). Based on probe **14**, probe **16** adds m-pyridine and pyridine units to replace benzene, which enhances the electron-absorbing properties and can be distinguished by the spectral changes at different detection intervals for sulfites and sulfides; it also provides good water solubility, and compared with the previous two probes that require the assistance of CTAB micelles, probe **16** can complete the reaction under PBS solvent. To solve the drawback of long reaction time, Sun [48] et al. introduced an additional carbon–carbon double bond to construct probe **17** based on probe **14**, which extended the π-conjugation relationship, reacted with SO_3^{2-}, significantly promoted the nucleophilic incorporation rate, shortened the probe conjugation structure, and advanced the response time to 30 min (Figure 1).

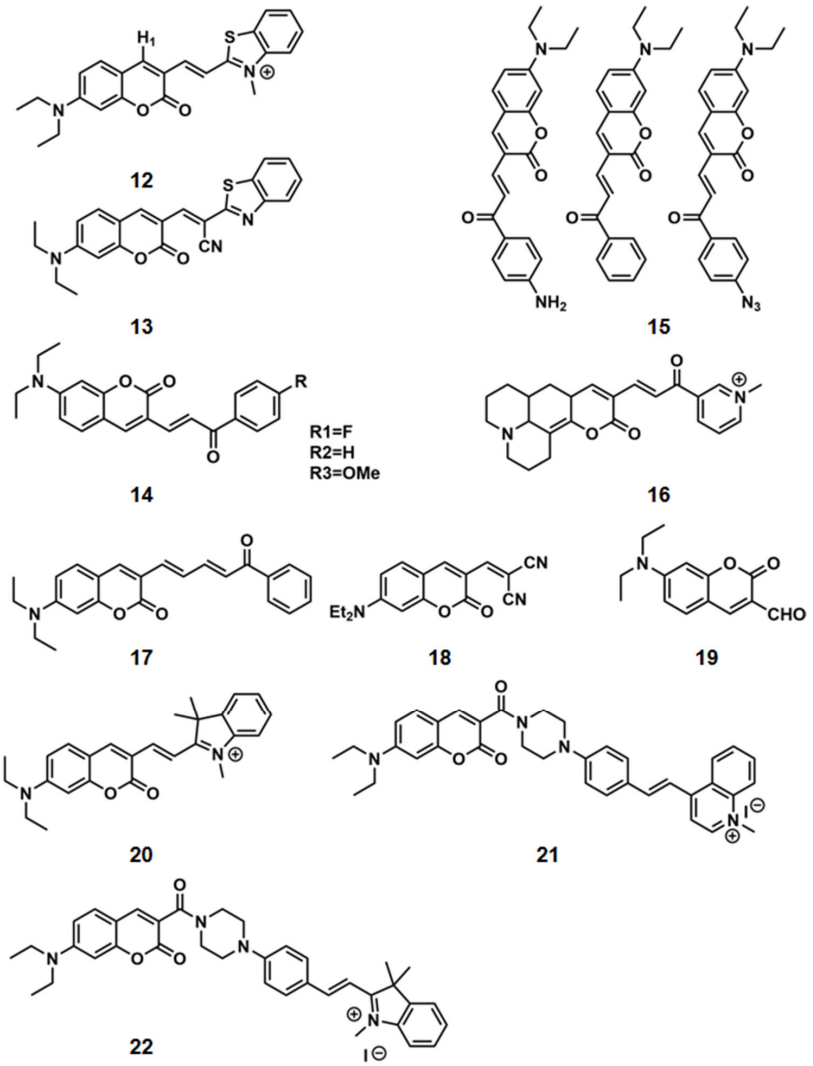

Scheme 5. The fabric of sulfite fluorescent probes **12**–**22**.

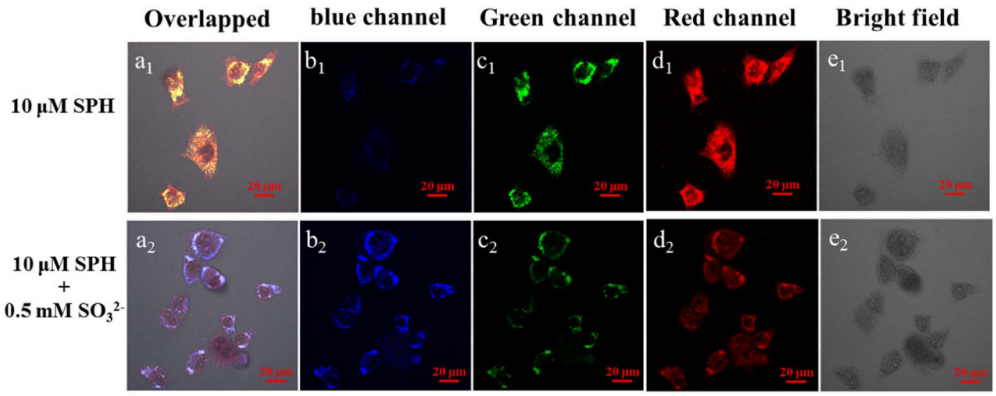

Figure 1. Fluorescence imaging of HeLa cells. Hela Cells incubated with 10 μM probe **17** for 30 min (**a**$_1$–**e**$_1$) and pretreated with 0.5 mM Na_2SO_3 for 30 min followed by incubation with 10 μM probe **11** for another 30 min (**a**$_2$–**e**$_2$). (**a**$_{1–2}$) merged of (**b**$_{1–2}$–**e**$_{1–2}$); (**b**$_{1–2}$) blue channel; (**c**$_{1–2}$) green channel; (**d**$_{1–2}$) red channel; (**e**$_{1–2}$) bright field; blue channel exited with a 404 nm laser; green and red channels excited with a 488 nm laser.

Probe **18** [49] and probe **19** [50] are both reactive probes. Probe **18** uses Michael addition to dicyano-vinyl group, which has high selectivity for sulfite and active sulfur. The reaction is completed within the 30 s. The detection mechanism of probe **19** is a special nucleophilic addition reaction with aldehydes. The optimum pH of this probe for detecting HSO_3^- is 5, which is not suitable for physiological environments. The detection limits of these two probes are too high, which limits their application.

Probes **20**–**22** are all mitochondrial-targetable. In 2015, Xu [51] et al. designed a probe with a detection limit of 90 nM and a response time of 3 min. This is the first probe that uses coumarin as a fluorophore and is localized to mitochondrial organelles. The probe not only showed a blue shift of 170 nm in the emission spectrum, but also two emission bands with good resolution after the addition of sulfite, which facilitated the fluorescence resolution (Figure 2). Yan's team designed probes **21** and **22** in 2019 and 2020, respectively [52,53]. Both probes are near-infrared emission-mitochondria-targeted fluorescent probes based on FRET and ICT platforms. Probe **21** has a large Stokes shift, high photostability, chemical stability, and thermal cycling ability, and enables realizing the differentiation of endogenous L02 cells and cancer cells. Probe **22**, based on probe **21**, was used for exogenous detection of HeLa cells and endogenous detection of HepG2 and L02 cells, and the study yielded the result that the endogenous HSO_3^-/SO_3^{2-} ratio detection can be successfully used to distinguish normal human cells and cancer cells. These mitochondria-targeting fluorescent probes have also made continuous breakthroughs in the detection limit.

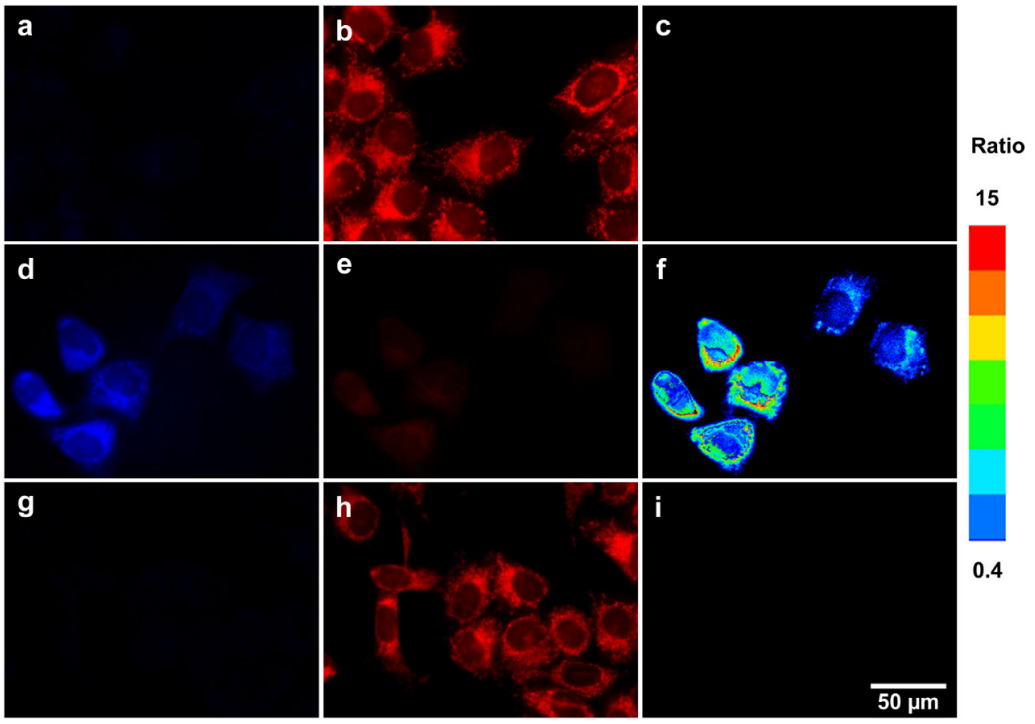

Figure 2. Fluorescence images of HeLa cells from the blue channel (scan range of 450–530 nm) and red channel (scan range of 600–700 nm) excited at 405 nm. (**a**,**b**) Fluorescence image of HeLa cells at the blue channel (**a**) and red channel (**b**) after incubation with probe **20** (2 mM) for 30 min; (**c**) Fluorescence ratio (Fblue/Fred) images of a and b. (**d**,**e**) Fluorescence image of HeLa cells treated with probe **20** (2 mM) for 30 min, and then further incubated with SO_2 donor (100 mM) for another 30 min; (**f**) Fluorescence ratio (Fblue/Fred) images (**d**,**e**); (**g**,**h**) Fluorescence image of HeLa cells treated with NEM (2 mM) and probe **20** (2 mM) for 30 min, and then incubated with synthetic SO_2 donor (100 mM) for another 30 min. Cells were observed at the blue channel (**g**) and red channel (**h**); (**i**) Fluorescence ratio (Fblue/Fred) images of g and h. (For interpretation of the references to colour in this figure legend, the reader is referred to the web version of this article).

2.2.2. PET Mechanisms

Photoelectron transfer refers to a class of fluorescent probes in which the recognition group and the fluorescent group are the electron donor and the electron acceptor, respectively, and the process of electron movement from the donor to the acceptor occurs, and this process usually causes the loss of fluorescence. When the recognition group is not bound to the target molecule, the electrons of the fluorescent group will leap to higher energy orbitals after being excited by light, making the electrons of the recognition group rapidly replenish the orbitals of the fluorescent group, while the electrons of its fluorescent group disappear from fluorescence because they cannot return to their original orbitals. When the recognition group binds to the target molecule, the PET process cannot be completed due to the decrease in electron-donating capacity, and the electrons on the fluorescent group can return to their original orbit, and fluorescence is restored (Scheme 6).

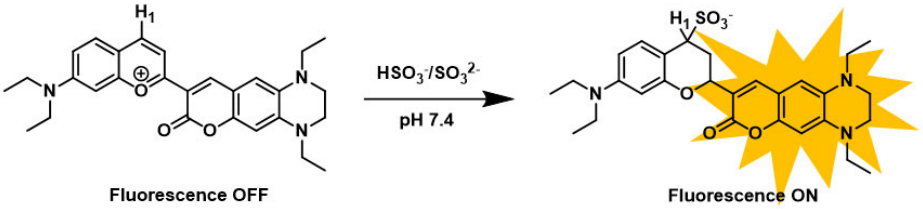

Scheme 6. Schematic diagram of mechanism PET.

Probes **23**–**25** developed based on coumarin-benzopyridine fluorophore and PET mechanisms have the following advantages: good water solubility and mitochondrial-targeting, and all three probes are turn-on type fluorescent probes. Probes **23** and **24** have very similar structures, differing in that these two probes have different groups at the carbon 7 position. The hydroxyl-containing probe **23** [54] has a longer emission wavelength and shows strong fluorescence emission at 600 nm when reacting with HSO_3^-/SO_3^{2-}. The experimental results indicate that probe **24** is more suitable for the detection of HSO_3^-/SO_3^{2-} in some water and food samples. Compared to probe **24**, probe **23** [55] can detect HSO_3^-/SO_3^{2-} inside and outside the cell because probe **23** has a lower detection limit. It is worth mentioning that the probe responds instantaneously to fluorescence, and the fluorescence signal starts immediately after the addition of 0.4 equiv. of HSO_3^- and can be stabilized within 15 s. On the contrary, the reaction time of probe **25** [56] with HSO_3^- was 30 s and the detection limit was 42 nM, which was a mediocre performance compared to the other two probes.

2.2.3. FRET Mechanisms

Ratiometric fluorescent probes **26**–**29** were designed based on FRET mechanisms. For biological applications, all of these probes can be used for intracellular imaging, and probe **28** can also be used for intra-mouse imaging. In terms of response time, probes **28** and **29** reacted with the SO_2 derivatives for only a few periods. However, probes **26** and **27** required 1 h.

In 2015, Dai's [57] group constructed the first two-photon ratiometric fluorescent probe **26** with a LOD of 53 nM in PBS buffer solution for single-photon excitation and 110 nm in PBS buffer solution for two-photon excitation.

In 2016, Zhao's [58] group reported probe **27**, which has the potential to be used for differentiation of hepatocellular carcinoma cells and normal cells, incubated HepG2 cells and L02 cells with the probe, respectively, and found that only HepG2 showed significant changes in fluorescence after incubation with the probe. However, the response time of this probe to detect HSO_3^- takes 1 h, limiting its application. To address this problem, Yang's [59] group constructed probe **28**, the first donor structure to construct benzoic acid as a FRET fluorescent probe. The probe can reach stability with SO_3^{2-}/HSO_3^- reaction within 3 min and has a Stokes shift of 239 nm. Importantly, probe **28** can detect SO_2 derivatives in mice (Figure 3).

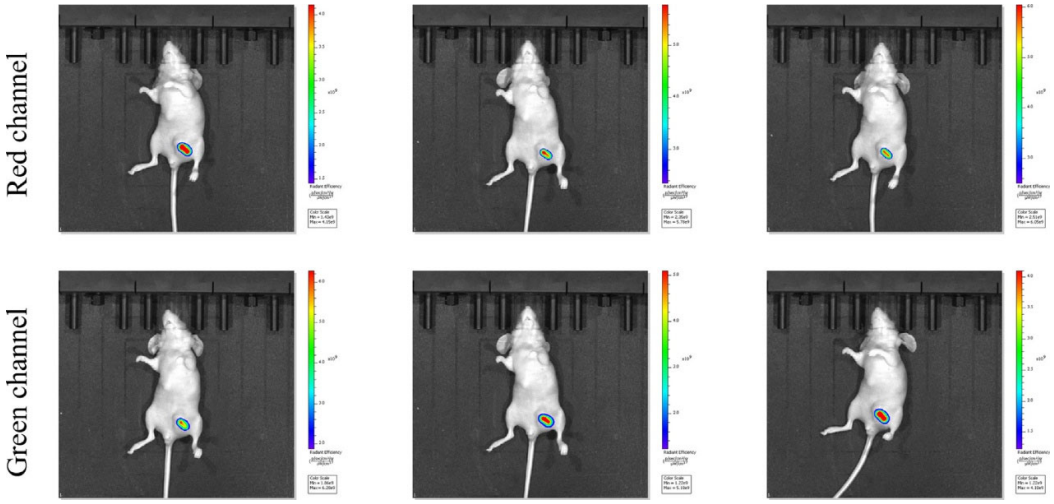

Figure 3. In vivo fluorescence imaging of probe **28** (10 μM) with Na_2SO_3 (100 μM) in HepG2 tumor-bearing nude mice at 0, 5, and 15 min. Reproduced with permission from Ref. [59]. Copyright (2021) Elsevier.

Recently, Ye's [60] group investigated the metabolism of Cys to SO_3^{2-}/HSO_3^- in mitochondria, and probe **29** is expected to be an effective tool for this purpose. Probe **29** detects SO_3^{2-}/HSO_3^- by dual-channel imaging in MCF-7 cells. Besides, LOD = 26.3 nM, which is lower than all the probes mentioned above (Scheme 7).

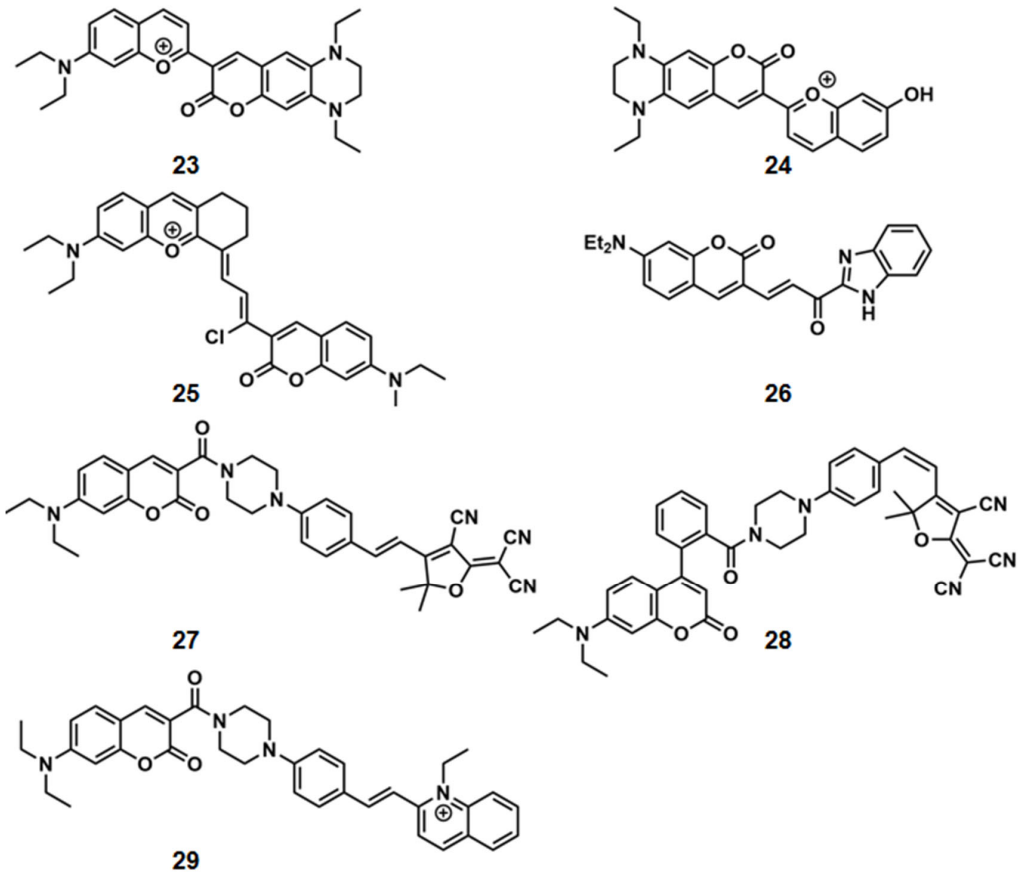

Scheme 7. The framework of sulfite fluorescent probes **23**–**29**.

2.3. Based on Hemicyanine Fluorophore

Hemicyanine stems are a series of anionic probes containing anthocyanin dyes due to their long emission wavelength, potential over-fluorescence, specific binding sites, and good water solubility [61]. Hemicyanine fluorophores can capture nucleophilic reagents via 1,2—addition or 1,4—addition [62,63]. We classified hemicyanine fluorophore into the following categories based on the mechanism including intramolecular charge transfer (ICT), and fluorescence resonance energy transfer (FRET).

2.3.1. ICT Mechanisms

Based on ICT mechanisms, probes **30**–**42** were exploited. In general, probes **31**, **32**, **38**, **40**, **42** were turn-on type, probes **30**, **33**–**37**, **39**, **41** are ratiometric type.

In 2014, Sun [61] et al. developed probe **30** based on hemicyanine dye, which can detect HSO_3^- in a 100% aqueous medium with a fast response time (within 90 s), and two well-separated emission peaks ($\Delta\lambda$ = 106 nm) can be obtained before and after the addition of HSO_3^-, and they prepared a simple and rapid test paper for the detection of HSO_3^-.

In 2016, Samanta [64] et al. developed a multifunctional fluorescent probe **31** with highly sensitive dual recognition sensing of SO_3^{2-} and SO_4^{2-}/HSO_4^-. The sensing mechanism of probe **31** for the anion SO_3^{2-} is essentially due to the breakage of the conjugate extension limiting the ICT, which in turn leads to the fluorescence on response. In contrast, the presence of SO_4^{2-}/HSO_4^- introduces the aggregation-induced emission (AIE) phenomenon to the system, which results in a turn-on fluorescence response. However, the detection limit of this probe was high (LOD = 106 nM). To further optimize it, in 2017, Yu [65] et al. developed a fluorescent probe capable of detecting SO_3^{2-}/HSO_3^- and HSO_4^- simultaneously using different emission channels. The detection limit of this probe was as low as 2.82 nM.

Because the positive charge of the anthocyanine derivatives can be localized to mitochondria, probes **33**–**36** had mitochondrial targeting. As shown by Scheme 8, probe **33** [66] was a symmetrical semicarbazide structure that allows the probe to undergo two nucleophilic addition reactions with HSO_3^-, thus enabling the detection of large concentrations of HSO_3^-/SO_3^{2-} and is the probe with the fastest response time (<30 s). In 2017, Yang [67] et al. developed two ratiometric probes **34a** and **34b** based on the electron-poor double bond structure. They studied the spectral properties of both probes and found that **34a** has an emission at 568 nm, while **34b** has an emission at 644 nm. This result leads to the conclusion that the emission spectra appear red shifted with the extension of the double bond. Additionally, the probe was used for fluorescence ratio imaging of endogenous HSO_3^- in BT-474 cells to detect endogenous sodium bisulfite. Probe **35** [68] allows for real-time monitoring of SO_3^{2-}/HSO_3^-. In 2021, Lin [69] et al., based on the semicarbazide backbone, developed three probes **36a**, **36b**, and **36c** (see figure Scheme 8). **36a** is a ratiometric probe with LOD = 0.27 mM and a response time of 50 min, and **36b** is a turn-on probe with LOD = 38.41 nM and a response time of 20 min, and the localization experiment found that the probe not only can localize to mitochondria but also have co-localization ability to Golgi apparatus, endoplasmic reticulum and other cell organelles.

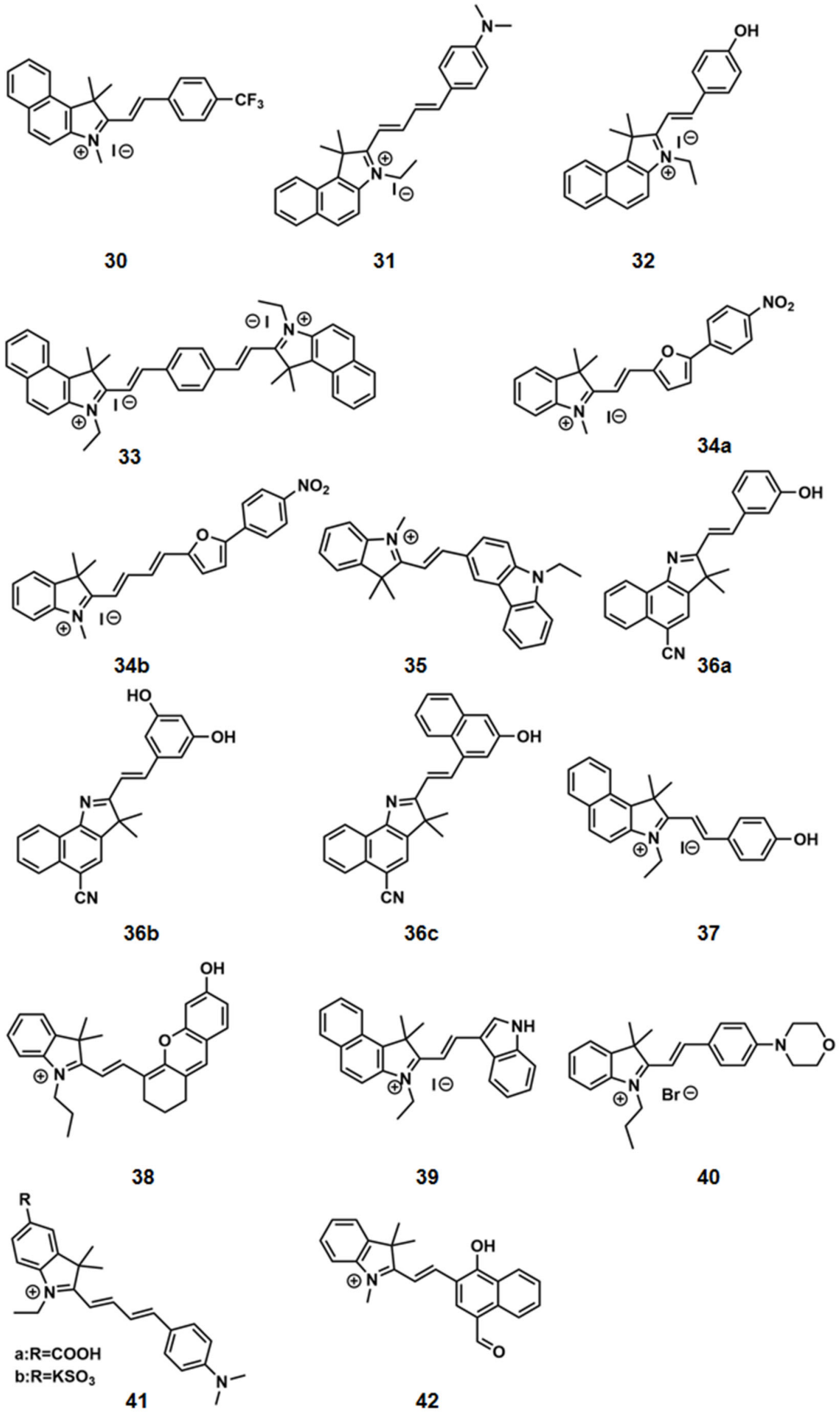

Scheme 8. The formation of sulfite fluorescent probes **30**–**42**.

In 2019, Qin's group [70] developed a ratiometric fluorescent probe **37** that reacted with 500 μM SO_3^{2-} and the color of the solution changed significantly from pink to colorless, probe **37** has the advantages of low LOD, high sensitivity, and high selectivity in HepG2 cells, and detects SO_3^{2-}/HSO_3^- reaction very quickly (within 60 s). In contrast to probe **37**, probe **38** [71] applied HSO_3^- fluorescence imaging in live mice, which was the first time used for imaging BALB/c mice to detect SO_3^{2-}/HSO_3^- in live mice.

In 2020, the Wang'group [72] and Zhou'group [73] designed probes **39** and **40**, respectively, for bisulfite detection. Probe **39** is a ratiometric fluorescent probe that eliminates background interference and has a detection limit of 80 nM. The probe reacts rapidly with bisulfite and reaches stability within 2 min. In contrast to probe **39**, the turn-on probe **40** was able to monitor bisulfite in real time (reaction completed within 30 s), and, the probe was imaged in vivo in live mice, and the results suggest that the probe can be used for the detection of bisulfite in serum of live mice. Meanwhile, in the study of Pan et al. [74], probes **41a** and **41b** with the molecular structure as shown in the Scheme 8 were designed. Both probes have a large Stokes shift (250 nm), and it was shown that **41a** containing carboxyl group responded more significantly to the fluorescence intensity change of HSO_3^- in pure water than **41b** containing sulfoxide group, and **41a** has lower cytotoxicity and better biocompatibility compared to **41b** for the detection of HSO_3^- in living cells, in addition to better response characteristics. However, when performing the optimization of the assay conditions, it was found that the assay was affected by the pH environment. To solve this problem, Shi [75] et al. designed to probe **42** with good acid and alkaline resistance within pH 3–11.

2.3.2. FRET Mechanisms

Probes **43**–**46** were developed based on FRET mechanisms, where **43** is the turn-on type and **44**–**46** is the ratiometric type. The detection limit of probe **44** is 0.78 nM, the response time of probe **45** is 2 min, probe **46** has lipid droplet targeting, and probe **43** is a two-photon fluorescent probe.

In 2016, Zhu [76] et al. first reported a two-photon fluorescent probe **43** for imaging SO_2 derivatives in biological tissues. The authors chose the acetyl fraction as the two-photon donor and the semicarbazone derivative as the quencher and recognition unit. Nuclear magnetic resonance spectroscopy and mass spectrometry demonstrated that the probe reacts with HSO_3^- to disrupt the conjugate structure and the HOMO-LUMO energy gap of the semicarbazide derivative energy receptor increases, inhibiting the FRET process. Notably, probe **43** was successfully applied with the detection of HSO_3^-/SO_3^{2-} imaging in HepG2 cells and rat liver tissue sections.

In 2018, Zhang's [77] group constructed probe **44**, which detects exogenous SO_3^{2-} in HeLa cells, and successfully detected cysteine metabolism in BRL cells. However, incubation of the probe with cells requires 4 h, limiting its application. Probe **45** [78] can detect HSO_3^-/SO_3^{2-} "naked eye" with large Stokes shift (260 nm). However, the experimental results found that GSH, Hcy, and Cys can affect the detection.

Lipid droplets are dynamic subcellular structures of lipid metabolism, and lipid droplet abnormalities are associated with a variety of diseases such as obesity, fatty liver, and cardiovascular disease. Recently, Lin's [79] group constructed probe **46**, which favors lipid droplets, the first probe constructed in concert with the FRET and ICT fluorescence platforms. Importantly, probe **46** successfully detected exogenous SO_2 derivatives of HeLa cells and endogenous SO_2 derivatives of HepG2 and L02, which are important for monitoring exogenous and endogenous HSO_3^-/SO_3^{2-} and even diagnosing cancer cells.

2.4. Based on Quinoline Fluorophore

Tryptamine quinoline, as a typical ICT dye, has a large Stokes shift. Turn-on fluorescent probes **47**–**50** were designed based on quinoline and its derivatives, with probe **47** had mitochondrial-targeting and probe **49** had two-photon properties.

The mitochondria-targeted fluorescent probe **47** [80] has fluorescence emission in the near-infrared and is stable in the pH 3–10 range in response to SO_3^{2-}/HSO_3^-; however, the probe takes up to 2 h to enter the cell when detecting SO_3^{2-}/HSO_3^- in HepG2 cells and zebrafish (Figure 4). It is known that background interference increases with longer detection cycles. In 2018, Xu's group [81] designed probe **48** for this problem based on quinoline derivatives, which have an ester head and a dimethylamine tail in the structure of probe **48**, both of which have good cell permeability. Confocal fluorescence imaging performed to detect SO_3^{2-} within HeLa cells showed that the probe was able to enter the cells within 2 min, largely shortening the detection time and reducing background interference. In addition, the authors also verified the low toxicity of probe **48** in HeLa, HEK293T, A549, and L02 cells of each cell.

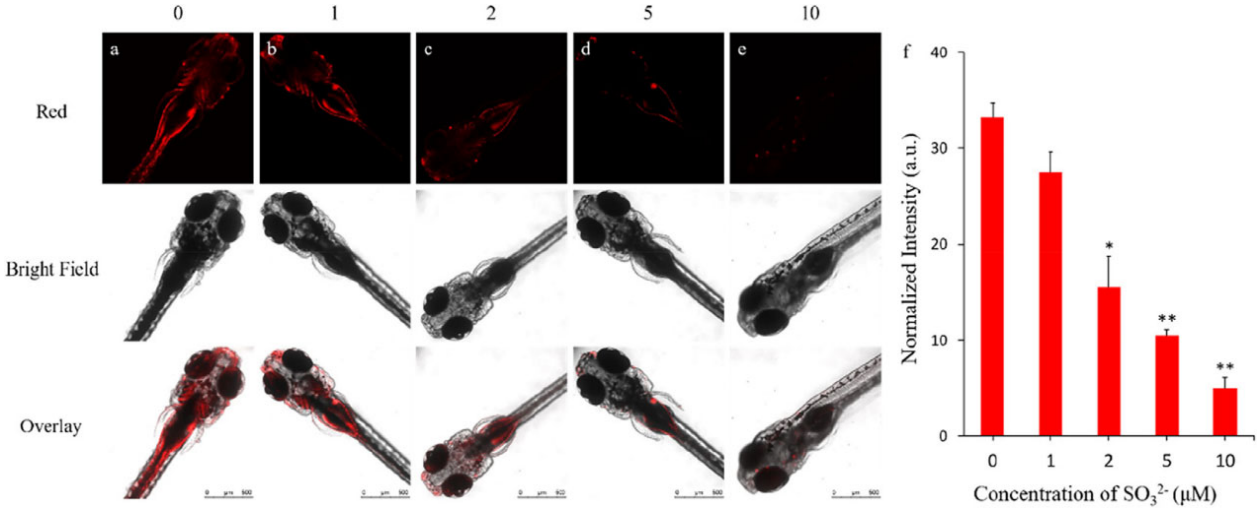

Figure 4. Imaging of SO_3^{2-} in zebrafish by probe **47**. The zebrafish were stained with (**a**) 2 μM probe **47** for 30 min; (**b**) 1 μM SO_3^{2-} for 30 min, 2 μM probe **47** for 30 min; (**c**) 2 μM SO_3^{2-} for 30 min, 2 μM probe **47** for 30 min; (**d**) 5 μM SO_3^{2-} for 30 min, 2 μM probe **47** for 30 min; (**e**) 10 μM SO_3^{2-} for 30 min, 2 μM probe **47** for 30 min. (**f**) Different normalized intensities toward different concentrations of SO_3^{2-}, respectively. Red channel: λex = 552 nm λem = 600–660 nm. Values are the means ± SD for each group of three experiments; * $p < 0.05$, ** $p < 0.01$. Reproduced with permission from Ref. [80]. Copyright (2020) Elsevier.

In 2019, Zhang [82] et al. designed probe **49** to reveal the two-photon nature of tryptamine quinoline derivatives for the first time, and secondly, probe **49** introduces β-chlorovinyl aldehyde as a reaction site with the introduction of halogen, which retains the reaction properties of the aldehyde group with SO_2 derivatives while introducing halogen for higher selectivity for thiol species. Compared with single photons, the two-photon penetration depth is stronger penetration, so the probe reacts with SO_2 derivatives extremely fast (<5 s). To demonstrate the utility of the probe, the authors successfully used it for two-photon imaging of SO_2 derivatives in live zebrafish.

In 2019, Zhou [83] et al. developed probe **50** using the mechanism of nucleophilic addition reaction of HSO_3^- with *α*,*β*—unsaturated C=C. Probe **50** is a responsive fluorescent probe with a long emission wavelength of 598 nm and also has the advantages of fast response time, low detection limit, high sensitivity, and high selectivity (Scheme 9).

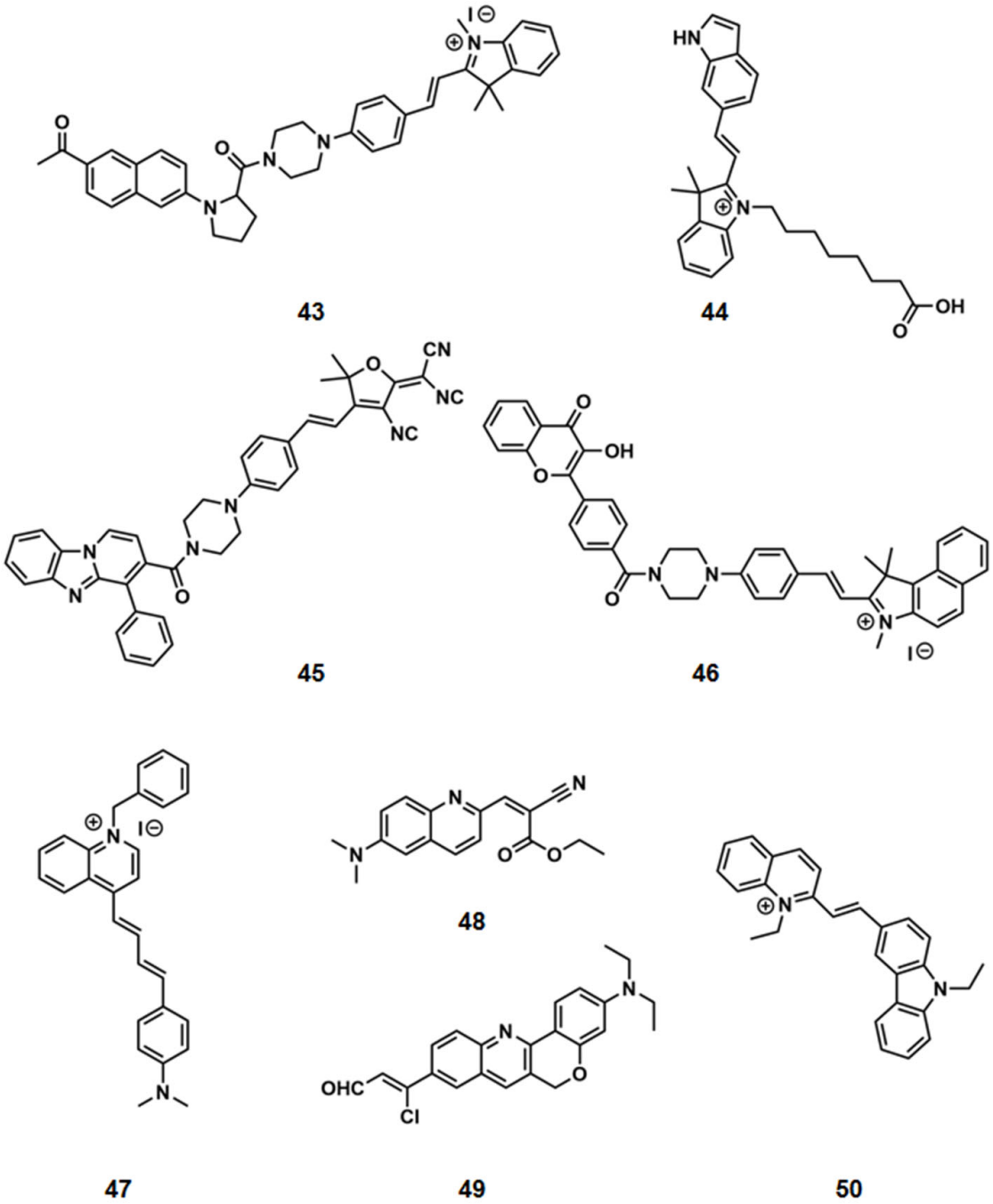

Scheme 9. Illustrations of sulfite fluorescent probes **43**–**50**.

2.5. Based on Naphthalimide Fluorophore

2.5.1. ICT Mechanisms

Probes **51**–**54** were designed based on naphthalimide and its derivatives, where **52** is the turn-on type and **51** and **53**–**54** are the ratiometric types.

Hou's group [84] and Zhang's group [85] developed probes **51** using 4-hydroxynaphtha limide and levulinic acid in 2013 and 2014, respectively, and Hou investigated the sensing properties, selectivity, sensitivity, pH, and utility of the probes for HSO_3^- in HEPES-buffered. Furthermore, Zhang et.al studied the spectral response, response time, sensitivity, selectivity, and utility of the probe for HSO_3^- in ethanol and water (3:7). All proved that probe **51** is a good tool for the detection of HSO_3^-.

Abnormal SO_2 levels further impair local immune function by affecting the amount and activity of lysosomal enzymes in macrophages, so it is important to monitor acidic

lysosomal SO_2 levels in biological systems. In 2017, Li's group [86] proposed a fluorescent probe **52** with lysosomal targeting consisting of a morpholine unit, a semicyanine, and a naphthalimide fluorophore, and the probe **52** exhibits intense fluorescence emission at 524 nm only in the presence of both SO_2 and H^+. This is an AND-logic-based design concept. Besides, probe **52** has the advantages of high selectivity, fast response, and very low detection limit.

Reactive oxygen is a single-electron reduction product of molecular oxygen, and the dose, type, location, and duration of reactive oxygen species differ in the effects they cause on cells. HSO_3^- is crucial as an antioxidant in regulating the balance of redox status in cells. Therefore, the monitoring of HSO_3^-/ROS (reactive oxygen) is of great interest. In 2021, probes **53** and **54** were proposed based on naphthalimide, respectively. Probe **53** designed by Wang [87] et al. is a reversible fluorescent probe that can be used to evaluate the redox state of HSO_3^-/H_2O_2 modulation in vitro and in vivo. Probe **53** itself can produce strong fluorescence emission at 580 nm, and after the C=C nucleophilic addition reaction with HSO_3^-, the fluorescence at 580 nm gradually decreases, and the strong fluorescence is emitted at 510 nm. Furthermore, the nucleophilic addition product can be oxidized by H_2O_2 to form the original C=C of the probe, and the fluorescence at 580 nm is re-enhanced. Moreover, HSO_3^-/H_2O_2 imaging was successfully performed in adult zebrafish and nude mice. Unlike probe **53**, probe **54** was proposed to identify HSO_3^- and ClO^- by Wu [88] et al. Using different emission channels, probe **54** caused strong fluorescence emission at 515 nm when interacting with ClO^- and at 548 nm when interacting with HSO_3^-. In addition, the selectivity experiments showed that the probe has high selectivity and strong anti-interference ability. Notably, the authors successfully detected HSO_3^- and ClO^- in plasma using probe **54** and performed intracellular imaging. The probe was also able to recognize endogenous ClO^- in vitro, thus distinguishing tumor cells and normal tissue cells.

2.5.2. ESIPT Mechanisms

The C=N isomerization could be inhibited by an intramolecular N–H...N–C hydrogen bond, the formation of hydrogen bonds can limit intramolecular rotation and rigidify the molecular structure, thus helping to minimize the nonradiative energy loss of the exciton and maximize the probability of its radiative leap (open emission). This interaction has been successfully applied to the design of AIE and ESIPT fluorescent materials. Turn-on fluorescent probes **55**, **56** were designed based on ESIPT mechanisms.

In 2012, Sun's [89] group reported for the first time the naphthalimide derivative probe **55** for the detection of HSO_3^- content in white sugar, and the reaction products of probe **55** with HSO_3^- were determined. Fluorescence titration and absorption titration experiments showed that probe **55** has good response properties. Recently, Huo [90] et al. constructed a probe **56** with the same structure, and probe **56** could detect SO_3^{2-} in HeLa cells and mice while being able to localize to the lysosome with a response time of the 30 s (Figure 5).

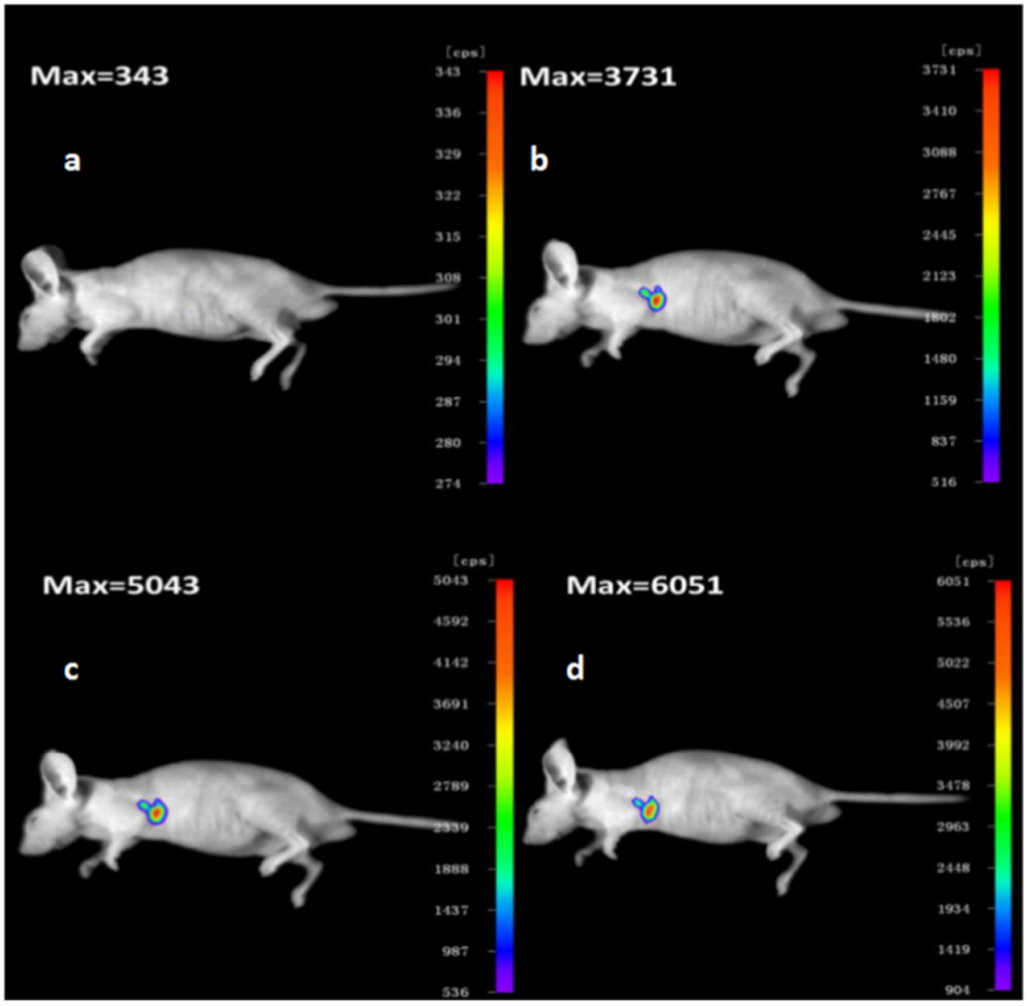

Figure 5. (**a**) mice were incubated with probe **56** (10 μM) for 30 min; (**b**) mice were incubated with probe **56** (10 μM) for 30 min and Na_2SO_3 (50 μM) 5 min; (**c**) mice were incubated with probe **56** (10 μM) for 30 min and Na_2SO_3 (50 μM) 10min; (**d**) mice were incubated with probe **56** (10 μM) for 30 min and Na_2SO_3 (50 μM) 25 min. Reproduced with permission from Ref. [90]. Copyright (2019) Elsevier.

2.6. Based on Benzimidazole Fluorophore

Probes **57**–**60** were designed based on benzimidazole and its derivatives, of which **60** were turn-on type and **57**–**59** were ratiometric type.

Back in 2011, probe **57** [91] was designed based on the selective reaction of SO_3^{2-} with aldehydes. The reaction of probe **57** with SO_3^{2-} can be stabilized within 5 min, and the detection range for SO_3^{2-} is 2–200 μmol/L. Earlier developed probes had many shortcomings, and Wang et al. studied the sensing response of the probe to bisulfite in an ethanol and acetate buffer solution at pH 4.6 (20 mmol/L), thus limiting the detection of probe **57** in a physiological environment. Thus, after continuous progress, Niu [92] et al. designed probe **58** for DMF/PBS at pH = 7.4, and probe **58** emits at 664 nm, which is due to its molecular structure of 2-(2-hydroxy-phenyl)-benzoimidazole(HBN)-CHO and TCF (2-dicyanmethylene-3-cyano-4,5,5-trimethyl-2,5dihydrofuran) combined by unsaturated C=C bonds, which can red shift emission, and importantly, probe **58** successfully detected BEL-7402 intracellular and exogenous SO_2 derivatives.

In 2019, Kavitha's group [93] designed a probe **59** using phenanthrene imidazole as a fluorescent group with the advantages of high selectivity and fast response. The authors concluded by fluorescence, ^{1}H NMR, and ESI-mass spectrometry studies that the mechanism of interaction of probe **59** with SO_3^{2-} is based on the nucleophilic addition of

carbon-carbon double bonds, blocking the π-conjugation. Moreover, the probe successfully monitored SO_3^{2-} in real samples and HeLa cells.

The dicyanovinyl group is a group with strong electron-absorbing properties, which can reduce the electron density of the carbon–carbon double bond and therefore is easy to undergo nucleophilic addition reactions. Probe **60** [94] was developed based on the dicyanovinyl group and the maleimide moiety to separate bisulfite and thiol amino acids. The study examined the absorption spectra and fluorescence emission spectra of the probe with sodium bisulfite and thiol amino acids, and both observed changes in the spectra, but differed in the time at which the changes occurred; these changes were observed approximately 30 min after the addition of thiol amino acids, whereas in the case of sodium bisulfite, the changes were observed immediately. More importantly, probe **60** measures the level of HSO_3^- in HeLa cells (Scheme 10).

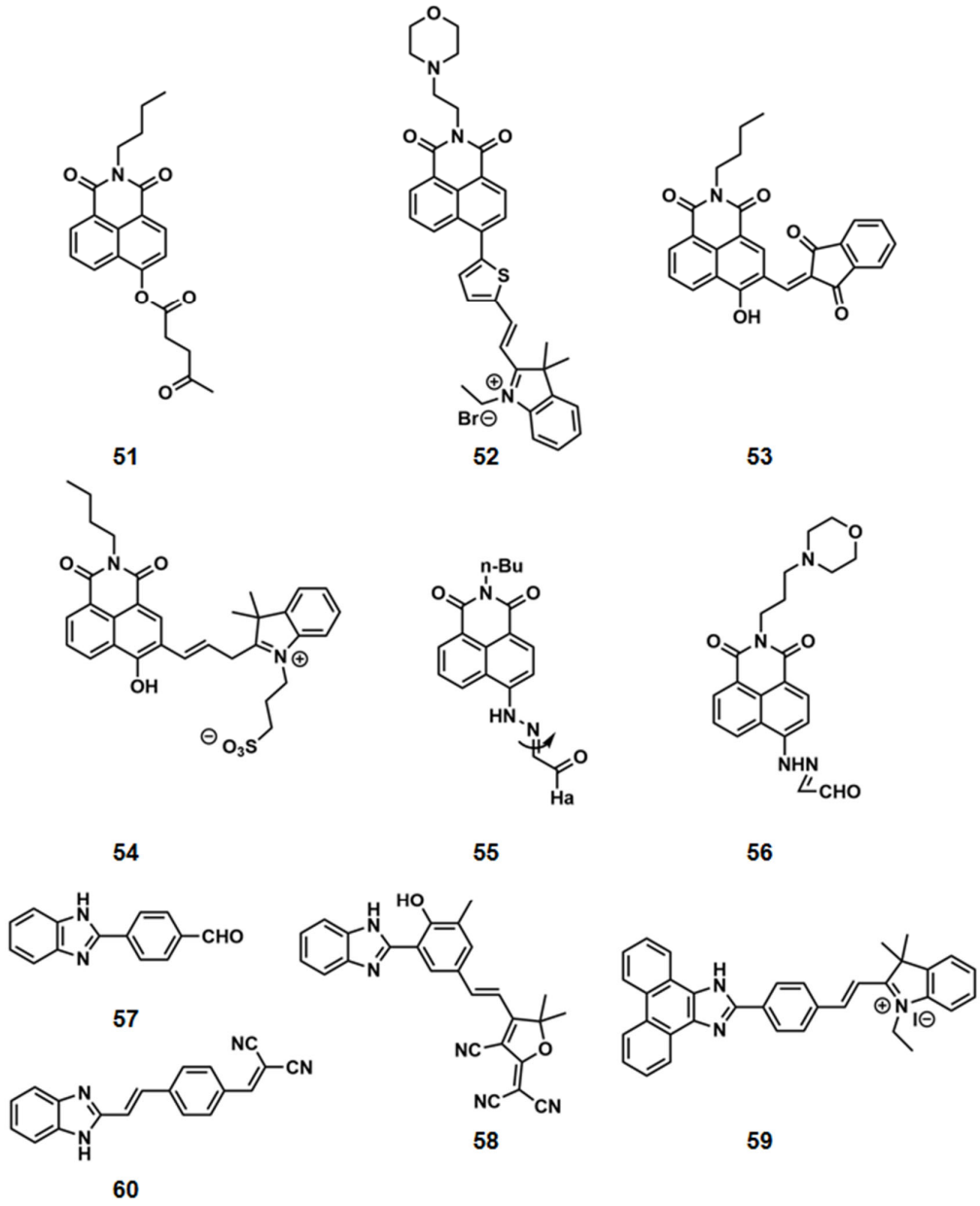

Scheme 10. Illustrations of sulfite fluorescent sensing **51**–**60**.

2.7. Based on Imidazole Fluorophore

The imidazopyridine derivatives have good photophysical properties, large Stokes shift, good photostability, and high fluorescence quantum yields. In 2019, Chen [95] et al. synthesized turn-on probes **61** using imidazopyridine derivatives as fluorescent agents and malononitrile moieties as SO_3^{2-} reactive sites, probe **61** has the advantages of large Stokes shift, high sensitivity degree, and high selectivity, and successfully determined SO_3^{2-} in MCF-7 cells and zebrafish (Figure 6).

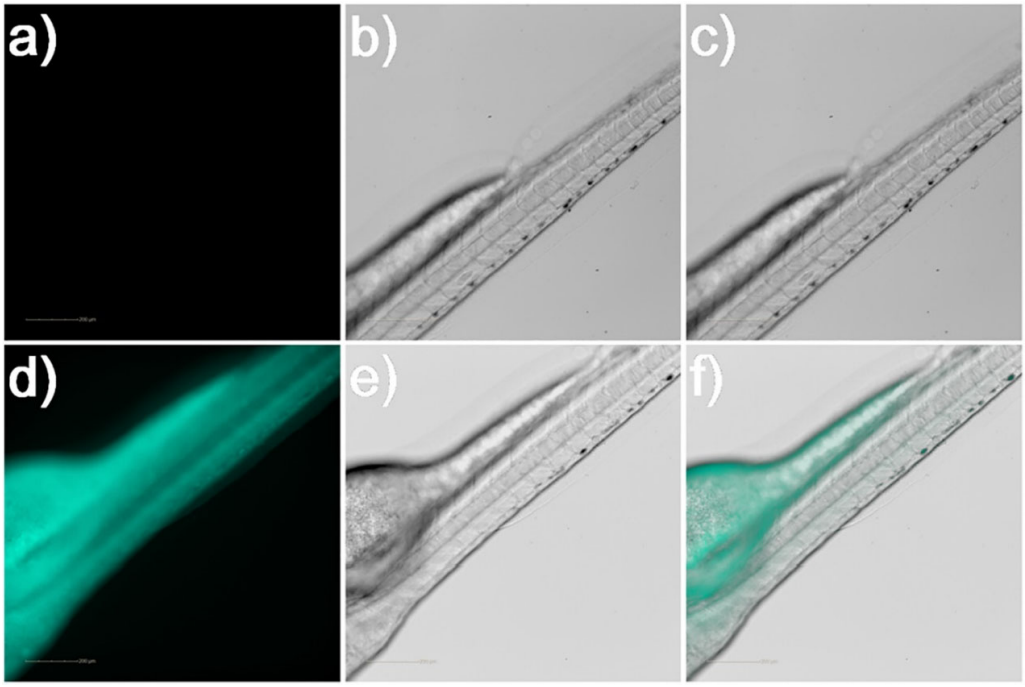

Figure 6. Fluorescence (**a**,**d**), Bright field (**b**,**e**) and merged (**c**,**f**) images of zebrafish. Top row (**a**–**c**): only seeded with probe **61** for 30 min. Bottom row, (**d**–**f**): pre-trained with SO_3^{2-} for 30 min and then seeded with probe **61** for 30 min.

2.8. Based on Triphenylamine Fluorophore

The ratiometric fluorescent probe **62** [96], a dual-channel chemosensor with both fluorescence and colorimetric response, is designed with an electron-rich triphenylamine-thiophene as the fluorophore and electron-donating group and an aldehyde group as the electron acceptor. With the increase of HSO_3^- concentration, the maximum emission wavelength of probe **62** was shifted from 560 nm to 440 nm, and at the same time, the color changed from yellow to colorless. It is worth mentioning that the experimental results demonstrate that the addition reaction of an aldehyde with HSO_3^- is reversible.

2.9. Based on Thiophene Fluorophore

Thiophenes are ideal building blocks for the synthesis of conjugated π-systems [97]. In 2021, Wang [98] et al. synthesized probes **63** with thienyl-substituted diketopyrrolopyrrole. They investigated HSO_3^- detection and imaging by probe **63** in normal hepatocytes and hepatocellular carcinoma cells, and found that there is a difference in endogenous HSO_3^- production by HepG2 and L02 cells, and the concentration of endogenous HSO_3^- in HepG2 cells is much higher than that in L02 cells, which is important for the diagnosis of hepatocellular carcinoma.

2.10. Based on Pyrene Fluorophore

Pyrene and its derivatives are important compounds with a huge conjugation system and stable photophysical properties [99,100]. Therefore, they are often used as fluorophores to design fluorescent probes for the recognition of anions, cations, and neutral small molecules.

In 2021, Chao's [101] group constructed a probe **64** based on pyrene derivatives. The results of mass spectrometry and infrared spectroscopy experiments showed that the reaction mechanism of probe **64** with SO_3^{2-} was the nucleophilic attack of unsaturated carbon–carbon double bonds in the $\alpha,\beta-$keto structure by SO_3^{2-}. More notably, endogenous SO_3^{2-} could be detected in HepG2 cells.

2.11. Based on Julolidine Fluorophore

In 2018, Yao's [102] group designed a ratiometric fluorescent probe **65** that successfully detected SO_3^{2-} within HepG2 and L929 cells and was able to localize to mitochondria. The experimental results show that probe **65** detects SO_3^{2-} in a two-step reaction, first adding in the C=N bond to shorten the conjugate structure of the probe, and then an intramolecular rearrangement occurs to further shorten the conjugate structure, resulting in a significant blue shift in the absorption and emission spectra. In 2019, Tamima's [103] group designed a ratiometric fluorescent probe **66** that successfully detected SO_2 derivatives in HeLa cells and was able to localize them to lysosomes. Probe **66** is based on the linear shape of the benzopyran dye system, which is a π-extended pyrroline system. Probe **66** has the following advantages: emission in the near-infrared wavelength range, the ability of the morpholine group in the structure to act as a partial quencher of PET, two-photon excitation, fully spectrally separated scale imaging, high sensitivity, and selectivity.

2.12. Based on Ir(III) Complex Fluorophore

Due to the high photoluminescence efficiency, long lifetime, and significant Stokes, bis-cyclometalated Ir(III) complex are increasingly used for the detection of analytes. In 2018, Gao's group [104] constructed the turn-on fluorescent probe **67**. Probe **67** has the typical characteristics of Ir(III) complexes, and upon interaction with HSO_3^-, the probe absorbs at 377, 408, and 466 nm. Meanwhile, probe **67** can selectively detect HSO_3^-, and the experimental results found that HSO_3^- is mainly present as SO_3^{2-} when the pH is close to neutral, but SO_3^{2-} does not respond to the probe.

2.13. Based on Rhodamine Fluorophore

In 2019, Liu's [105] group reported a rhodamine probe **68** based on the Michael addition reaction. Probe **68** enables the detection of SO_3^{2-} levels in HepG2 cells. The probe itself had two emission peaks at 450 nm and 566 nm, respectively, and the fluorescence intensity at 566 nm gradually decreased with the addition of SO_3^{2-} and remained unchanged at 450 nm. The response time of this probe to sulfite is completed within the 30 s, which is better than some of the fluorescent probes reported so far.

2.14. Based on Flavor Fluorophore

In 2015, Xu [106] et al. constructed a probe **69** capable of detecting HSO_3^- and Al^{3+} simultaneously, enabling the simultaneous detection of negative ions and cations by a single probe. However, the results of competitive and selective experiments show that Fe^{3+}, Cu^{2+}, and Mn^{2+} have some influence on the detection and poor selectivity. This design concept has great significance, but it needs continuous improvement (Scheme 11).

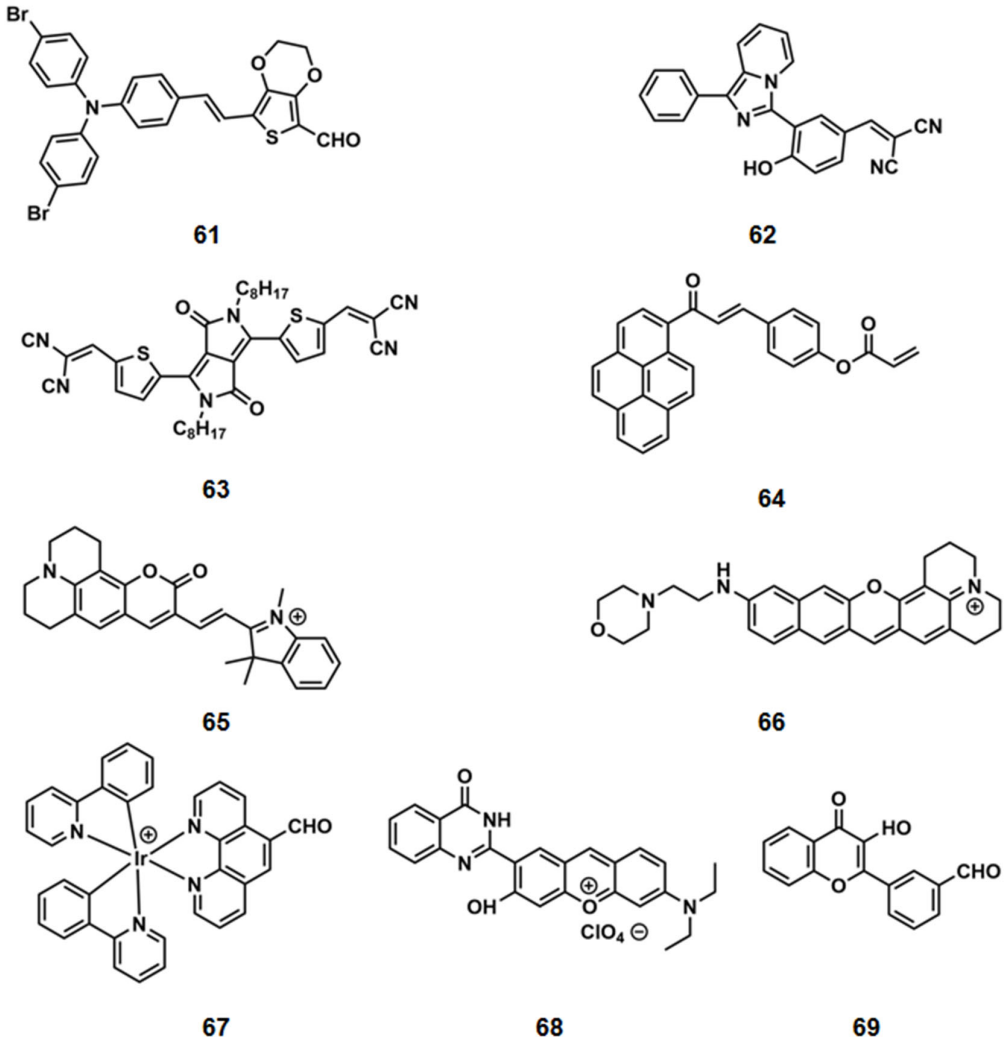

Scheme 11. Typical structure diagram of sulfite fluorescent probes **61**–**69**.

3. Conclusions and Prospect

People are increasingly concerned about diet and health, and sulfite, as a common food antioxidant additive and preservative, can also be produced endogenously and is closely related to peoples' daily life, so it is necessary to develop a simple, efficient, and inexpensive testing instrument. In the past decade, sulfite fluorescent probes have developed rapidly. This paper reviews the research progress of sulfite small-molecule fluorescent probes in the last decade.

We found that the probes constructed based on the ICT mechanism are the most basic and extensive. Researchers are continuously studying the composition of fluorescent groups with recognition groups and linkage bonds. For the first 5 years, mostly single-emission turn-on fluorescent probes were also used only to detect sulfite components in real samples (e.g., water, sugar, wine). In the latter 5 years, ratiometric fluorescent probes have been continuously developed for their advantages. More and more excellent fluorophores were also explored and gradually applied to image endogenous sulfites in cells, tissues, zebrafish, and mouse models. In addition, fluorescent probes with organelle (e.g., mitochondria, lysosomes, lipid droplets) targeting, two-photon, and reversible cycling have been introduced. Importantly, the response time of fluorescent probes for sulfite reactions is getting shorter, the detection limits are getting lower, and the water solubility is getting better. More notably, in the past two years, scholars were keen to develop red or near-infrared ratiometric fluorescent probes with excellent analytical properties such as low background interference, low biological damage, and deep tissue penetration, which

are more suitable for in vivo imaging. However, a sulfite fluorescent probe that combines all the advantages is still being explored. Therefore, there are still the following challenges and difficulties in design and application: (1) When imaging sulfites in cells or tissues, the probe incubation time is slightly longer (>30 min), which is not conducive to application for real time monitoring in vivo. (2) The components in serum are complex and low, and the probes summarized do not currently detect sulfite concentrations in serum.

Combining the above advantages and disadvantages of sulfite small-molecule fluorescent probes, we believe that there is still much room for progress and development in this field. Future goals can be devoted to the construction of optical imaging of sulfite in vivo with low detection limits, high selectivity, no damage, stability in physiological environments, reversible cycling, and can be monitored in real time and used for sulfite.

Author Contributions: T.L.: conceptualization, investigation, writing—original draft, validation, visualization. X.C.: investigation, validation. K.W.: writing—review and editing. Z.H.: project administration, funding acquisition. All authors have read and agreed to the published version of the manuscript.

Funding: General Program of Jiangsu Health Commission (H2019069). This work is supported by the Major Projects of Precision Medicine of Wuxi Health Committee, China (No. J202001), the Top Talents Project of Wuxi Taihu Lake Talent Plan.

Institutional Review Board Statement: Not applicable.

Informed Consent Statement: Not applicable.

Data Availability Statement: No new data were created or analyzed in this study. Data sharing is not applicable to this article.

Conflicts of Interest: The authors declare that they have no known competing financial interests or personal relationships that could have appeared to influence the work reported in this paper.

References

1. Ghanbari, G.M.; Heibati, B.; Naddafi, K.; Kloog, I.; Oliveri, C.G.; Polosa, R.; Ferrante, M. Evaluation of Chronic Obstructive Pulmonary Disease (COPD) Attributed to Atmospheric O_3, NO_2, and SO_2 Using Air Q Model (2011–2012 Year). *Environ. Res.* **2016**, *144*, 99–105. [CrossRef] [PubMed]
2. Wang, X.; Tang, H.; Huang, X. Water-Soluble Fluorescent Probes for Bisulfite and Viscosity Imaging in Living Cells: Pyrene Vs. Anthracene. *Spectrochim. Acta A* **2021**, *260*, 119902. [CrossRef] [PubMed]
3. Vincent, A.S.; Lim, B.G.; Tan, J.; Whiteman, M.; Cheung, N.S.; Halliwell, B.; Wong, K.P. Sulfite-Mediated Oxidative Stress in Kidney Cells. *Kidney Int.* **2004**, *65*, 393–402. [CrossRef] [PubMed]
4. Yang, X.; Cui, Y.; Li, Y.; Zheng, L.; Xie, L.; Ning, R.; Liu, Z.; Lu, J.; Zhang, G.; Liu, C.; et al. A New Diketopyrrolopyrrole-Based Probe for Sensitive and Selective Detection of Sulfite in Aqueous Solution. *Spectrochim. Acta A* **2015**, *137*, 1055–1060. [CrossRef] [PubMed]
5. Tavallali, H.; Deilamy-Rad, G.; Parhami, A.; Lohrasbi, S. A Novel and Simple Fluorescent and Colorimetric Primary Chemosensor Based On Congo-Red for Sulfite and Resultant Complex as Secondary Fluorescent Chemosensor Towards Carbonate Ions: Fluorescent Probe Mimicking INHIBIT Logic Gate. *Talanta* **2016**, *149*, 168–177. [CrossRef]
6. Lien, K.; Hsieh, D.P.H.; Huang, H.; Wu, C.; Ni, S.; Ling, M. Food Safety Risk Assessment for Estimating Dietary Intake of Sulfites in the Taiwanese Population. *Toxicol. Rep.* **2016**, *3*, 544–551. [CrossRef]
7. Bauchart-Thevret, C.; Stoll, B.; Burrin, D.G. Intestinal Metabolism of Sulfur Amino Acids. *Nutr. Res. Rev.* **2009**, *22*, 175–187. [CrossRef]
8. Yang, X.; Feng, P.; Ma, L.; Kang, T.; Hu, S.; Hai, A.; Ke, B.; Liu, J.; Li, M. Biological Applications of a Turn-On Bioluminescent Probe for Monitoring Sulfite Oxidase Deficiency in vivo. *Eur. J. Med. Chem.* **2020**, *200*, 112476. [CrossRef]
9. Ghorai, A.; Mondal, J.; Chandra, R.; Patra, G.K. A Reversible Fluorescent-Colorimetric Imino-Pyridyl Bis-Schiff Base Sensor for Expeditious Detection of Al^{3+} and HSO_3^- in Aqueous Media. *Dalton T.* **2015**, *44*, 13261–13271. [CrossRef]
10. Deng, Z.; Li, F.; Zhao, G.; Yang, W.; Hu, Y. A Mitochondrion-Targeted Dual-Site Fluorescent Probe for the Discriminative Detection of SO_3^{2-} and HSO_3^- in Living HepG-2 Cells. *RSC Adv.* **2020**, *10*, 26349–26357. [CrossRef]
11. Xu, J.; Yuan, H.; Zeng, L.; Bao, G. Recent Progress in Michael Addition-Based Fluorescent Probes for Sulfur Dioxide and its Derivatives. *Chin. Chem. Lett.* **2018**, *29*, 1456–1464. [CrossRef]
12. Li, K.; Li, L.; Zhou, Q.; Yu, K.; Kim, J.S.; Yu, X. Reaction-Based Fluorescent Probes for SO2 Derivatives and their Biological Applications. *Coordin. Chem. Rev.* **2019**, *388*, 310–333. [CrossRef]

13. Kalimuthu, P.; Tkac, J.; Kappler, U.; Davis, J.J.; Bernhardt, P.V. Highly Sensitive and Stable ElectroChemical Sulfite Biosensor Incorporating a Bacterial Sulfite Dehydrogenase. *Anal. Chem.* **2010**, *82*, 7374–7379. [CrossRef]
14. Wang, R.; Wang, R.; Ju, D.; Lu, W.; Jiang, C.; Shan, X.; Chen, Q.; Sun, G. "ON–OFF–ON" Fluorescent Probes Based On Nitrogen-Doped Carbon Dots for Hypochlorite and Bisulfite Detection in Living Cells. *Anal.* **2018**, *143*, 5834–5840. [CrossRef]
15. Dalaman, U.; Özdoğan, H.; Sircan, A.K.; Şengül, S.A.; Yaraş, N. Sulfur Dioxide Derivative Prevents the Prolongation of Action Potential During the Isoproterenol-Induced Hypertrophy of Rat Cardiomyocytes. *Anacad. Bras. Cienc.* **2021**, *93*, e20201664. [CrossRef]
16. Liang, J.; Liu, L.; Kang, X.; Hu, F.; Mao, L. Mechanism Underlying the Effect of SO_2-Induced Oxidation on Human Skin Keratinocytes. *Medicine* **2020**, *99*, e23152. [CrossRef]
17. Zhu, Z.; Zhang, L.; Chen, Q.; Li, K.; Yu, X.; Tang, C.; Kong, W.; Jin, H.; Du, J.; Huang, Y. Macrophage-Derived Sulfur Dioxide is a Novel Inflammation Regulator. *Biochem. Bioph. Res. Co.* **2020**, *524*, 916–922. [CrossRef]
18. Tan, L.; Lin, W.; Zhu, S.; Yuan, L.; Zheng, K. A Coumarin-Quinolinium-Based Fluorescent Probe for Ratiometric Sensing of Sulfite in Living Cells. *Org. Biomol. Chem.* **2014**, *12*, 4637. [CrossRef]
19. Li, Q.; Nie, J.; Shan, Y.; Li, Y.; Du, J.; Zhu, L.; Yang, Q.; Bai, F. Water-Soluble Fluorescent Probe for Simultaneous Detection of Cyanide, Hypochlorite and Bisulfite at Different Emission Wavelengths. *Anal. Bioanal. Chem.* **2020**, *591*, 113539. [CrossRef]
20. Yang, B.; Xu, J.; Zhu, H.L. Recent Progress in the Small-Molecule Fluorescent Probes for the Detection of Sulfur Dioxide Derivatives (HSO3-/SO32-). *Free Radical Bio. Med.* **2019**, *145*, 42–60. [CrossRef]
21. Shangguan, M.; Jiang, X.; Lu, Z.; Zou, W.; Chen, Y.; Xu, P.; Pan, Y.; Hou, L. A Coumarin-Based Fluorescent Probe for Hypochlorite Ion Detection in Environmental Water Samples and Living Cells. *Talanta* **2019**, *202*, 303–307. [CrossRef] [PubMed]
22. Ma, C.; Zhang, F.; Wang, Y.; Zhu, X.; Liu, X.; Zhao, C.; Zhang, H. Synthesis and Application of Ratio Fluorescence Probe for Chloride. *Anal. Bioanal. Chem.* **2018**, *410*, 6507–6516. [CrossRef] [PubMed]
23. Xu, Z.; Shi, W.; Yang, C.; Xu, J.; Liu, H.; Xu, J.; Zhu, B. A Colorimetric Fluorescent Probe for Rapid and Specific Detection of Nitrite. *Luminescence* **2019**, *35*, 299–304. [CrossRef] [PubMed]
24. Zhang, Y.; Zhang, L. Designed Multifunctional Ratiometric Fluorescent Probe for Directly Detecting Fluoride Ion/Dichromate and Indirectly Monitoring Urea. *J. Hazard. Mater.* **2021**, *418*, 126271. [CrossRef] [PubMed]
25. Hou, L.; Li, F.; Guo, J.; Zhang, X.; Kong, X.; Cui, X.T.; Dong, C.; Wang, Y.; Shuang, S. A Colorimetric and Ratiometric Fluorescent Probe for Cyanide Sensing in Aqueous Media and Live Cells. *J. Mater. Chem. B* **2019**, *7*, 4620–4629. [CrossRef] [PubMed]
26. Cheng, S.; Sun, R.; Wu, Z.; Mei, H.; Yang, H.; Kong, Q.; Xu, K. A Novel Reversible Fluorescent Probe for Cu^{2+} and S^{2-} ions and Imaging in Living Cells. *Methods Appl. Fluores.* **2022**, *10*, 035009. [CrossRef]
27. Kim, J.; Lee, S.; Han, M.S. pH-Guided Fluorescent Sensing Probe for the Discriminative Detection of Cl^- and Br^- in Human Serum. *Anal. Chim. Acta* **2022**, *1210*, 339879. [CrossRef]
28. Choi, M.G.; Hwang, J.; Eor, S.; Chang, S. Chromogenic and Fluorogenic Signaling of Sulfite by Selective Deprotection of Resorufin Levulinate. *Org. Lett.* **2010**, *12*, 5624–5627. [CrossRef]
29. Zha, Y.; Xin, R.; Zhang, M.; Cui, X.; Li, N. Stimuli-Responsive Azobenzene-Quantum Dots for Multi-Sensing of Dithionite, Hypochlorite, and Azoreductase. *Microchim. Acta* **2020**, *187*, 481. [CrossRef]
30. Wang, J.; Hao, Y.; Wang, H.; Yang, S.; Tian, H.; Sun, B.; Liu, Y. Rapidly Responsive and Highly Selective Fluorescent Probe for Bisulfite Detection in Food. *J. Agr. Food Chem.* **2017**, *65*, 2883–2887. [CrossRef]
31. Zhang, Y.; Guan, L.; Yu, H.; Yan, Y.; Du, L.; Liu, Y.; Sun, M.; Huang, D.; Wang, S. Reversible Fluorescent Probe for Selective Detection and Cell Imaging of Oxidative Stress Indicator Bisulfite. *Anal. Chem.* **2016**, *88*, 4426–4431. [CrossRef]
32. Li, H. Rapidly Responsive and Highly Selective Fluorescent Probe for Sulfite Detection in Real Samples and Living Cells. *Anal. Chim. Acta* **2015**, *897*, 102–108. [CrossRef]
33. Zhang, W.; Liu, T.; Huo, F.; Ning, P.; Meng, X.; Yin, C. Reversible Ratiometric Fluorescent Probe for Sensing Bisulfate/H_2O_2 and its Application in Zebrafish. *Anal. Chem.* **2017**, *89*, 8079–8083. [CrossRef]
34. Ye, Z.; Duan, C.; Sheng, R.; Xu, J.; Wang, H.; Zeng, L. A Novel Colorimetric and Ratiometric Fluorescent Probe for Visualizing SO_2 Derivatives in Environment and Living Cells. *Talanta* **2018**, *176*, 389–396. [CrossRef]
35. Liu, X.; Yang, Q.; Chen, W.; Mo, L.; Chen, S.; Kang, J.; Song, X. A Ratiometric Fluorescent Probe for Rapid, Sensitive and Selective Detection of Sulfur Dioxide with Large Stokes Shifts by Single Wavelength Excitation. *Org. Biomol. Chem.* **2015**, *13*, 8663–8668. [CrossRef]
36. Qi, F.; Zhang, F.; Mo, L.; Ren, X.; Wang, Y.; Li, X.; Liu, X.; Zhang, Y.; Yang, Z.; Song, X. A benzothiazole-Based Bifunctional Fluorescent Probe for the Ratiometric Detection of Fluoride and Sulphite in Real Samples. *Spectrochim. Acta A* **2019**, *219*, 547–551. [CrossRef]
37. Jia, X.; Yang, Y.; Zhai, H.; Zhang, Q.; He, Y.; Liu, Y.; Liu, Y. The Mechanisms of a Bifunctional Fluorescent Probe for Detecting Fluoride and Sulfite Based On Excited-State Intramolecular Proton Transfer and Intramolecular Charge Transfer. *Struct. Dynam.* **2021**, *8*, 34103. [CrossRef]
38. Zhang, H.; Huang, Z.; Feng, G. Colorimetric and Ratiometric Fluorescent Detection of Bisulfite by a New benzothiazole-Hemicyanine Hybrid. *Anal. Chim. Acta* **2016**, *920*, 72–79. [CrossRef]
39. Zhang, J.; Peng, A.; Lv, Y.; Zhang, Y.; Wang, X.; Zhang, G.; Tian, Z. A Colorimetric Fluorescent Probe for SO_2 Derivatives-Bisulfite and Sulfite at Nanomolar Level. *J. Fluoresc.* **2017**, *27*, 1767–1775. [CrossRef]

40. Ren, H.; Huo, F.; Wu, X.; Liu, X.; Yin, C. An ESIPT-Induced NIR Fluorescent Probe to Visualize Mitochondrial Sulfur Dioxide During Oxidative Stress in vivo. *Chem. Commun.* **2021**, *57*, 655–658. [CrossRef]
41. Peng, M.; Yang, X.; Yin, B.; Guo, Y.; Suzenet, F.; En, D.; Li, J.; Li, C.; Duan, Y. A Hybrid Coumarin-Thiazole Fluorescent Sensor for Selective Detection of Bisulfite Anions *in Vivo* and in Real Samples. *Chem. Asian J.* **2014**, *9*, 1817–1822. [CrossRef] [PubMed]
42. Sun, Y.; Chen, Z.; Chen, F.; Liu, H.; He, H.; Zhang, X.; Wang, S. An benzothiazole-Based Near-Infrared Fluorescent Probe for Colorimetric and Ratiometric Detection of Bisulfite and its Application in Living Cells. *J. Fluoresc.* **2017**, *27*, 1405–1411. [CrossRef] [PubMed]
43. Sun, Y.; Liu, J.; Zhang, J.; Yang, T.; Guo, W. Fluorescent Probe for Biological Gas SO_2 Derivatives Bisulfite and Sulfite. *Chem. Commun.* **2013**, *49*, 2637. [CrossRef] [PubMed]
44. Wang, J.; Long, L.; Xiao, X. A Fast-Responsive Fluorescent Probe for Sulfite and its Bioimaging. *Luminescence* **2016**, *31*, 775–781. [CrossRef] [PubMed]
45. Tian, H.; Qian, J.; Sun, Q.; Bai, H.; Zhang, W. Colorimetric and Ratiometric Fluorescent Detection of Sulfite in Water Via Cationic Surfactant-Promoted Addition of Sulfite to α,β-Unsaturated Ketone. *Anal. Chim. Acta* **2013**, *788*, 165–170. [CrossRef] [PubMed]
46. Tian, H.; Qian, J.; Sun, Q.; Jiang, C.; Zhang, R.; Zhang, W. A Coumarin-Based Fluorescent Probe for Differential Identification of Sulfide and Sulfite in CTAB Micelle Solution. *Analyst* **2014**, *139*, 3373. [CrossRef]
47. Pei, X.; Tian, H.; Zhang, W.; Brouwer, A.M.; Qian, J. Colorimetric and Fluorescent Determination of Sulfide and Sulfite with Kinetic Discrimination. *Analyst* **2014**, *139*, 5290–5296. [CrossRef]
48. Sun, Q.; Zhang, W.; Qian, J. A Ratiometric Fluorescence Probe for Selective Detection of Sulfite and its Application in Realistic Samples. *Talanta* **2017**, *162*, 107–113. [CrossRef]
49. Wu, M.; He, T.; Li, K.; Wu, M.; Huang, Z.; Yu, X. A Real-Time Colorimetric and Ratiometric Fluorescent Probe for Sulfite. *Analyst* **2013**, *138*, 3018. [CrossRef]
50. Cheng, X.; Jia, H.; Feng, J.; Qin, J.; Li, Z. "Reactive" Probe for Hydrogen Sulfite: "Turn-On" Fluorescent Sensing and Bioimaging Application. *J. Mater. Chem. B* **2013**, *1*, 4110. [CrossRef]
51. Xu, W.; Teoh, C.L.; Peng, J.; Su, D.; Yuan, L.; Chang, Y. A Mitochondria-Targeted Ratiometric Fluorescent Probe to Monitor Endogenously Generated Sulfur Dioxide Derivatives in Living Cells. *Biomaterials* **2015**, *56*, 1–9. [CrossRef]
52. Yan, Y.; He, X.; Miao, J.; Zhao, B. A Near-Infrared and Mitochondria-Targeted Fluorescence Probe for Ratiometric Monitoring of Sulfur Dioxide Derivatives in Living Cells. *J. Mater. Chem. B Mater. Biol. Med.* **2019**, *7*, 6585–6591. [CrossRef]
53. Yan, Y.H.; Wu, Q.R.; Che, Q.L.; Ding, M.M.; Xu, M.; Miao, J.Y.; Zhao, B.X.; Lin, Z.M. A Mitochondria-Targeted Fluorescent Probe for the Detection of Endogenous SO_2 Derivatives in Living Cells. *Analyst* **2020**, *145*, 2937–2944. [CrossRef]
54. Zhong, K.; Yao, Y.; Sun, X.; Wang, Y.; Tang, L.; Li, X.; Zhang, J.; Yan, X.; Li, J. Mitochondria-Targeted Fluorescent Turn-On Probe for Rapid Detection of Bisulfite/Sulfite in Water and Food Samples. *J. Agr. Food Chem.* **2022**, *70*, 5159–5165. [CrossRef]
55. Chen, W.; Fang, Q.; Yang, D.; Zhang, H.; Song, X.; Foley, J. Selective, Highly Sensitive Fluorescent Probe for the Detection of Sulfur Dioxide Derivatives in Aqueous and Biological Environments. *Anal. Chem.* **2015**, *87*, 609–616. [CrossRef]
56. Zhang, Y.; Zhang, X.; Yang, X.F.; Zhang, J. A Colorimetric and Fluorogenic Probe for Bisulfite Using Benzopyrylium as the Recognition Unit. *Luminescence* **2017**, *32*, 1233–1239. [CrossRef]
57. Dai, X.; Zhang, T.; Du, Z.; Cao, X.; Chen, M.; Hu, S.; Miao, J.; Zhao, B. An Effective Colorimetric and Ratiometric Fluorescent Probe for Bisulfite in Aqueous Solution. *Anal. Chim. Acta* **2015**, *888*, 138–145. [CrossRef]
58. Wu, W.; Wang, Z.; Dai, X.; Miao, J.; Zhao, B. An Effective Colorimetric and Ratiometric Fluorescent Probe Based FRET with a Large Stokes Shift for Bisulfite. *Sci. Rep.* **2016**, *6*, 25315. [CrossRef]
59. Shen, W.; Xu, H.; Feng, J.; Sun, W.; Hu, G.; Hu, Y.; Yang, W. A Ratiometric and Colorimetric Fluorescent Probe Designed Based On FRET for Detecting SO_3^{2-}/HSO_3^- in Living Cells and Mice. *Spectrochim. Acta A* **2021**, *263*, 120183. [CrossRef]
60. Han, X.; Zhai, Z.; Yang, X.; Zhang, D.; Tang, J.; Zhu, J.; Zhu, X.; Ye, Y. A FRET-Based Ratiometric Fluorescent Probe to Detect Cysteine Metabolism in Mitochondria. *Org. Biomol. Chem.* **2020**, *18*, 1487–1492. [CrossRef]
61. Sun, Y.; Zhao, D.; Fan, S.; Duan, L.; Li, R. Ratiometric Fluorescent Probe for Rapid Detection of Bisulfite through 1,4-Addition Reaction in Aqueous Solution. *J. Agr. Food Chem.* **2014**, *62*, 3405–3409. [CrossRef] [PubMed]
62. Chen, Y.; Zhu, C.; Yang, Z.; Chen, J.; He, Y.; Jiao, Y.; He, W.; Qiu, L.; Cen, J.; Guo, Z. A Ratiometric Fluorescent Probe for Rapid Detection of Hydrogen Sulfide in Mitochondria. *Angew. Chem. Int. Edit.* **2013**, *52*, 1688–1691. [CrossRef] [PubMed]
63. Li, D.P.; Wang, Z.Y.; Cao, X.J.; Cui, J.; Wang, X.; Cui, H.Z.; Miao, J.Y.; Zhao, B.X. A Mitochondria-Targeted Fluorescent Probe for Ratiometric Detection of Endogenous Sulfur Dioxide Derivatives in Cancer Cells. *Chem. Commun.* **2016**, *52*, 2760–2763. [CrossRef] [PubMed]
64. Samanta, S.; Dey, P.; Ramesh, A.; Das, G. A Solo Fluorogenic Probe for the Real-Time Sensing of SO_3^{2-} and SO_4^{2-}/HSO_4^- in Aqueous Medium and Live Cells by Distinct Turn-On Emission Signals. *Chem. Commun.* **2016**, *52*, 10381–10384. [CrossRef] [PubMed]
65. Yu, T.; Yin, G.; Niu, T.; Yin, P.; Li, H.; Zhang, Y.; Chen, H.; Zeng, Y.; Yao, S. A Novel Colorimetric and Fluorescent Probe for Simultaneous Detection of SO_3^{2-}/HSO_3^- and HSO_4^- by Different Emission Channels and its Bioimaging in Living Cells. *Talanta* **2018**, *176*, 1–7. [CrossRef]
66. Zheng, X.; Li, H.; Feng, W.; Xia, H.; Song, Q. Two-Step Sensing, Colorimetric and Ratiometric Fluorescent Probe for Rapid Detection of Bisulfite in Aqueous Solutions and in Living Cells. *ACS Omega* **2018**, *3*, 11831–11837. [CrossRef]

67. Yang, Y.; Zhou, T.; Bai, B.; Yin, C.; Xu, W.; Li, W. Design of Mitochondria-Targeted Colorimetric and Ratiometric Fluorescent Probes for Rapid Detection of SO_2 Derivatives in Living Cells. *Spectrochim. Acta A* **2018**, *196*, 215–221. [CrossRef]
68. Shi, J.; Shu, W.; Tian, Y.; Wu, Y.; Jing, J.; Zhang, R.; Zhang, X. A Real-Time Ratiometric Fluorescent Probe for Imaging of SO_2 Derivatives in Mitochondria of Living Cells. *RSC Adv.* **2019**, *9*, 22348–22354. [CrossRef]
69. Lin, X.; Liu, W.; Xu, S.; Li, Z.; Zhang, H.; Yu, M. Imaging of Intracellular Bisulfate Based On Sensitive Ratiometric Fluorescent Probes. *Spectrochim. Acta A* **2022**, *265*, 120335. [CrossRef]
70. Qin, Y.; Jiang, X.; Que, Y.; Gu, J.; Wu, T.; Aihemaiti, A.; Shi, K.; Kang, W.; Hu, B.; Lan, J.; et al. A Ratiometric and Colorimetric Hemicyanine Fluorescent Probe for Detection of SO_2 Derivatives and its Applications in Bioimaging. *Molecules* **2019**, *24*, 4011. [CrossRef]
71. Li, D.; Tian, X.; Li, Z.; Zhang, J.; Yang, X. Preparation of a Near-Infrared Fluorescent Probe Based on IR-780 for Highly Selective and Sensitive Detection of Bisulfite-Sulfite in Food, Living Cells, and Mice. *J. Agr. Food Chem.* **2019**, *67*, 3062–3067. [CrossRef]
72. Wang, L.; Yang, W.; Song, Y.; Gu, Y.; Hu, Y. A Double-Indole Structure Fluorescent Probe for Monitoring Sulfur Dioxide Derivatives with Distinct Ratiometric Fluorescence Signals in Mammalian Cells. *Spectrochim. Acta A* **2020**, *225*, 117495. [CrossRef]
73. Zhou, R.; Cui, G.; Hu, Y.; Qi, Q.; Huang, W.; Yang, L. An Effective Biocompatible Fluorescent Probe for Bisulfite Detection in Aqueous Solution, Living Cells, and Mice. *RSC Adv.* **2020**, *10*, 25352–25357. [CrossRef]
74. Pan, X.; Cheng, S.; Zhang, C.; Qi, X. Two Highly Sensitive Fluorescent Probes Based On Cinnamaldehyde with Large Stokes Shift for Sensing of HSO_3^- in Pure Water and Living Cells. *Anal. Bioanal. Chem.* **2020**, *412*, 6959–6968. [CrossRef]
75. Shi, Q.; Shen, L.; Xu, H.; Wang, Z.; Yang, X.; Huang, Y.; Redshaw, C.; Zhang, Q. A 1-Hydroxy-2,4-Diformylnaphthalene-Based Fluorescent Probe and its Detection of Sulfites/Bisulfite. *Molecules* **2021**, *26*, 3064. [CrossRef]
76. Zhu, X.; Zhu, L.; Liu, H.; Hu, X.; Peng, R.; Zhang, J.; Zhang, X.; Tan, W. A Two-Photon Fluorescent Turn-On Probe for Imaging of SO_2 Derivatives in Living Cells and Tissues. *Anal. Chim. Acta* **2016**, *937*, 136–142. [CrossRef]
77. Xu, B.; Zhou, H.; Mei, Q.; Tang, W.; Sun, Y.; Gao, M.; Zhang, C.; Deng, S.; Zhang, Y. Real-Time Visualization of Cysteine Metabolism in Living Cells with Ratiometric Fluorescence Probes. *Anal. Chem.* **2018**, *90*, 2686–2691. [CrossRef]
78. Zhang, G.; Ji, R.; Kong, X.; Ning, F.; Liu, A.; Cui, J.; Ge, Y. A FRET Based Ratiometric Fluorescent Probe for Detection of Sulfite in Food. *RSC Adv.* **2019**, *9*, 1147–1150. [CrossRef]
79. Yan, Y.; Cui, X.; Li, Z.; Ding, M.; Che, Q.; Miao, J.; Zhao, B.; Lin, Z. A Synergetic FRET/ICT Platform-Based Fluorescence Probe for Ratiometric Imaging of Bisulfite in Lipid Droplets. *Anal. Chim. Acta* **2020**, *1137*, 47–55. [CrossRef]
80. Zeng, R.F.; Lan, J.S.; Wu, T.; Liu, L.; Liu, Y.; Ho, R.; Ding, Y.; Zhang, T. A Novel Mitochondria-Targetted Near-Infrared Fluorescent Probe for Selective and Colorimetric Detection of Sulfite and its Application in Vitro and Vivo. *Food Chem.* **2020**, *318*, 126358. [CrossRef]
81. Xu, J.; Zheng, D.J.; Su, M.M.; Chen, Y.C.; Jiao, Q.C.; Yang, Y.S.; Zhu, H.L. A Rapid Cell-Permeating Turn-On Probe for Sensitive and Selective Detection of Sulfite in Living Cells. *Org. Biomol. Chem.* **2018**, *16*, 8318–8324. [CrossRef] [PubMed]
82. Cai, F.; Hou, B.; Zhang, S.; Chen, H.; Ji, S.; Shen, X.C.; Liang, H. A Chromenoquinoline-Based Two-Photon Fluorescent Probe for the Highly Specific and Fast Visualization of Sulfur Dioxide Derivatives in Living Cells and Zebrafish. *J. Mater. Chem. B* **2019**, *7*, 2493–2498. [CrossRef] [PubMed]
83. Zhou, F.; Sultanbawa, Y.; Feng, H.; Wang, Y.; Meng, Q.; Wang, Y.; Zhang, Z.; Zhang, R. A New Red-Emitting Fluorescence Probe for Rapid and Effective Visualization of Bisulfite in Food Samples and Live Animals. *J. Agr. Food Chem.* **2019**, *67*, 4375–4383. [CrossRef] [PubMed]
84. Hou, P.; Chen, S.; Voitchovsky, K.; Song, X. A Colorimetric and Ratiometric Fluorescent Probe for Sulfite Based on an Intramolecular Cleavage Mechanism. *Luminescence* **2014**, *29*, 749–753. [CrossRef] [PubMed]
85. Liu, C.; Wu, H.; Yang, W.; Zhang, X. A Simple Levulinate-Based Ratiometric Fluorescent Probe for Sulfite with a Large Emission Shift. *Anal. Sci.* **2014**, *30*, 589–593. [CrossRef]
86. Li, J.; Sun, Y.; Wang, C.; Guo, Z.; Shen, Y.; Zhu, W. AND-Logic Based Fluorescent Probe for Selective Detection of Lysosomal Bisulfite in Living Cells. *Anal. Chem.* **2019**, *91*, 11946–11951. [CrossRef]
87. Wang, Y.; Zhou, F.; Meng, Q.; Zhang, S.; Jia, H.; Wang, C.; Zhang, R.; Zhang, Z. A Novel Fluorescence Probe for the Reversible Detection of Bisulfite and Hydrogen Peroxide Pair in vitro and in vivo. *Chem. Asian J.* **2021**, *16*, 3419–3426. [CrossRef]
88. Wu, L.; Qi, S.; Liu, Y.; Wang, X.; Zhu, L.; Yang, Q.; Du, J.; Xu, H.; Li, Y. A Novel Ratiometric Fluorescent Probe for Differential Detection of HSO_3^- and ClO^- and Application in Cell Imaging and Tumor Recognition. *Anal. Bioanal. Chem.* **2021**, *413*, 1137–1148. [CrossRef]
89. Sun, Y.; Wang, P.; Liu, J.; Zhang, J.; Guo, W. A Fluorescent Turn-On Probe for Bisulfite Based On Hydrogen Bond-Inhibited C = N Isomerization Mechanism. *Analyst* **2012**, *137*, 3430. [CrossRef]
90. Huo, F.; Wu, Q.; Yin, C.; Zhang, W.; Zhang, Y. A High Efficient and Lysosome Targeted "Off-On" Probe for Sulfite Based On Nucleophilic Addition and ESIPT. *Spectrochim. Acta A* **2019**, *214*, 429–435. [CrossRef]
91. Wang, G.; Qi, H.; Yang, X. A Ratiometric Fluorescent Probe for Bisulphite Anion, Employing Intramolecular Charge Transfer. *Luminescence* **2013**, *28*, 97–101. [CrossRef]
92. Niu, T.; Yu, T.; Yin, G.; Chen, H.; Yin, P.; Li, H. A Novel Colorimetric and Ratiometric Fluorescent Probe for Sensing SO_2 Derivatives and their Bio-Imaging in Living Cells. *Analyst* **2019**, *144*, 1546–1554. [CrossRef]

93. Venkatachalam, K.; Asaithambi, G.; Rajasekaran, D.; Periasamy, V. A Novel Ratiometric Fluorescent Probe for "Naked-Eye" Detection of Sulfite Ion: Applications in Detection of Biological SO_3^{2-} Ions in Food and Live Cells. *Spectrochim. Acta A* **2020**, *228*, 117788. [CrossRef]
94. Kolińska, J.; Grzelakowska, A. Novel Styrylbenzimidazolium-Based Fluorescent Probe for Reactive Sulfur Species: Selectively Distinguishing Between Bisulfite and Thiol Amino Acids. *Spectrochim. Acta A* **2021**, *262*, 120151. [CrossRef]
95. Chen, S.; Hou, P.; Sun, J.; Wang, H.; Liu, L. Imidazo[1,5-α]Pyridine-Based Fluorescent Probe with a Large Stokes Shift for Specific Recognition of Sulfite. *Spectrochim. Acta A* **2020**, *225*, 117508. [CrossRef]
96. Cheng, X.; He, P.; Zhong, Z.; Liang, G. Reaction-Based Probe for Hydrogen Sulfite: Dual-Channel and Good Ratiometric Response. *Luminescence* **2016**, *31*, 1372–1378. [CrossRef]
97. Mishra, A.; Ma, C.; Bäuerle, P. Functional Oligothiophenes: Molecular Design for Multidimensional Nanoarchitectures and their Applications. *Chem. Rev.* **2009**, *109*, 1141–1276. [CrossRef]
98. Wang, J.; Xu, W.; Wang, Y.; Hua, J. Diketopyrrolopyrrole-Based Fluorescent Probe for Endogenous Bisulfite Detection and Bisulfite Triggered Phototoxicity Specific in Liver Cancer Cells. *Spectrochim. Acta A* **2021**, *262*, 120098. [CrossRef]
99. Aparin, I.O.; Proskurin, G.V.; Golovin, A.V.; Ustinov, A.V.; Formanovsky, A.A.; Zatsepin, T.S.; Korshun, V.A. Fine Tuning of Pyrene Excimer Fluorescence in Molecular Beacons by Alteration of the Monomer Structure. *J. Org. Chem.* **2017**, *82*, 10015–10024. [CrossRef]
100. Matías, N.; Möller, A.D. Diffusion of Nitric Oxide and Oxygen in Lipoproteins and Membranes Studied by Pyrene Fluorescence Quenching. *Free Radic. Bio. Med.* **2018**, *4*, 553.
101. Chao, J.; Zhao, J.; Zhang, Y.; Huo, F.; Yin, C.; Li, M.; Duan, Y. High-Specific Fluorescence Probe for SO_3^{2-} Detection and Bioimaging. *J. Fluoresc* **2021**, *31*, 363–371. [CrossRef]
102. Yao, Y.; Sun, Q.; Chen, Z.; Huang, R.; Zhang, W.; Qian, J. A Mitochondria-Targeted Near Infrared Ratiometric Fluorescent Probe for the Detection of Sulfite in Aqueous and in Living Cells. *Talanta* **2018**, *189*, 429–436. [CrossRef]
103. Tamima, U.; Santra, M.; Song, C.W.; Reo, Y.J.; Ahn, K.H. A Benzopyronin-Based Two-Photon Fluorescent Probe for Ratiometric Imaging of Lysosomal Bisulfite with Complete Spectral Separation. *Anal. Chem.* **2019**, *91*, 10779–10785. [CrossRef]
104. Gao, H.; Qi, H.; Peng, Y.; Qi, H.; Zhang, C. Rapid "Turn-On" Photo Luminescence Detection of Bisulfite in Wines and Living Cells with a Formyl Bearing Bis-Cyclometalated Ir(III) Complex. *Analyst* **2018**, *143*, 3670–3676. [CrossRef]
105. Liu, Y.; Ren, T.B.; Cheng, D.; Hou, J.; Su, D.; Yuan, L. An ESIPT-Based Ratiometric Fluorescent Probe for Highly Sensitive and Rapid Detection of Sulfite in Living Cells. *ChemistryOpen* **2019**, *8*, 1251–1257. [CrossRef]
106. Xu, S.; Tang, R.; Wang, Z.; Zhou, Y.; Yan, R. A Novel Flavone-Based Fluorescent Probe for Relay Recognition of HSO_3^- and Al^{3+}. *Spectrochim. Acta A* **2015**, *149*, 208–215. [CrossRef]